Journal of Experimental Botany, Vol. 67, No. 8 pp. 2483–2494, 2016
doi:10.1093/jxb/erw065 Advance Access publication 29 February 2016

RESEARCH PAPER

The type 3 effector NopL of *Sinorhizobium* sp. strain NGR234 is a mitogen-activated protein kinase substrate

Ying-Ying Ge[1], Qi-Wang Xiang[1], Christian Wagner[1], Di Zhang[1], Zhi-Ping Xie[1,2,*] and Christian Staehelin[1,2,*]

[1] State Key Laboratory of Biocontrol and Guangdong Key Laboratory of Plant Resources, School of Life Sciences, Sun Yat-sen University, Guangzhou, China
[2] Shenzhen Research and Development Center of State Key Laboratory of Biocontrol, School of Life Sciences, Sun Yat-sen University, Baoan, Shenzhen, China

* Correspondence: xiezping@mail.sysu.edu.cn or cst@mail.sysu.edu.cn

Received 22 December 2015; Accepted 2 February 2016

Editor: Katherine Denby, University of Warwick

Abstract

Pathogenic bacteria utilize type 3 secretion systems to inject type 3 effectors (T3Es) into host cells, thereby subverting host defense reactions. Similarly, T3Es of symbiotic nitrogen-fixing rhizobia can affect nodule formation on roots of legumes. Previous work showed that NopL (nodulation outer protein L) of *Sinorhizobium* (*Ensifer*) sp. strain NGR234 is multiply phosphorylated in eukaryotic cells and that this T3E suppresses responses mediated by mitogen-activated protein (MAP) kinase signaling in yeast (mating pheromone signaling) and plant cells (expression of pathogenesis-related defense proteins). Here, we show that NopL is a MAP kinase substrate. Microscopic observations of fluorescent fusion proteins and bimolecular fluorescence complementation analysis in onion cells indicated that NopL is targeted to the nucleus and forms a complex with SIPK (salicylic acid-induced protein kinase), a MAP kinase of tobacco. *In vitro* experiments demonstrated that NopL is phosphorylatyed by SIPK. At least nine distinct spots were observed after two-dimensional gel electrophoresis, indicating that NopL can be hyperphosphorylated by MAP kinases. Senescence symptoms in nodules of beans (*Phaseolus vulgaris* cv. Tendergreen) were analyzed to determine the symbiotic effector activity of different NopL variants with serine to alanine substitutions at identified and predicted phosphorylation sites (serine–proline motif). NopL variants with six or eight serine to alanine substitutions were partially active, whereas NopL forms with 10 or 12 substituted serine residues were inactive. In conclusion, our findings provide evidence that NopL interacts with MAP kinases and reveals the importance of serine–proline motifs for effector activity during symbiosis.

Key words: Effector, mitogen-activated protein kinase, multiple phosphorylation, NopL, *Sinorhizobium* (*Ensifer*) sp. strain NGR234, type 3 protein secretion system.

Introduction

Mitogen-activated protein (MAP) kinase cascades play pivotal roles in the induction of various plant defense reactions (Meng and Zhang, 2013; Zhao *et al.*, 2014). Activation of defense-related MAP kinase signaling pathways depends on pattern recognition receptors, which recognize structurally conserved microbial elicitors, so-called pathogen-associated molecular patterns (PAMPs) (Boller and Felix, 2009; Macho and Zipfel, 2014). However, many phytopathogenic Gram-negative bacteria can antagonize PAMP-triggered defense responses by employing type 3 protein secretion systems (T3SSs) that deliver toxin-like type 3 effectors (T3Es) into plant cells. Various T3Es contribute to bacterial virulence by targeting specific components of defense pathways, such as pattern recognition receptors, proteins of MAP kinase

pathways, and transcription factors (Hann *et al.*, 2010; Feng and Zhou, 2012; Macho and Zipfel, 2015). To counteract T3Es, plants have evolved defense mechanisms that are induced by direct recognition of T3Es (avirulence proteins) or detection of T3E-triggered cellular changes. These processes depend on specific host resistance (R) proteins and often culminate in local apoptosis [i.e. a hypersensitive response (HR)]. In this way, growth of biotrophic pathogens in the necrotic tissue is arrested (effector-triggered immunity) (Jones and Dangl, 2006; Gassmann and Bhattacharjee, 2012).

Rhizobia are symbiotic bacteria that reduce atmospheric nitrogen to ammonia in special root organs of legumes, the so-called nodules. The fixed nitrogen is then provided to the host plant in exchange for photosynthetically assimilated carbon compounds and other nutrients. Nodule formation is the result of a bacterial infection process, which depends on signals produced by both symbiotic partners. In response to flavonoids that are secreted by host legumes, rhizobia produce lipo-chitooligosaccharidic nodulation signals (Nod factors), which are perceived by specific plant receptors (LysM receptor kinases). Nod factor-induced signaling in host plants triggers expression of symbiotic plant genes required for bacterial infection and nodule initiation (Perret *et al.*, 2000; Ferguson *et al.*, 2010; Oldroyd, 2013). In addition to Nod factors, rhizobia secrete other symbiotic determinants such as surface polysaccharides and T3Es (Nops, nodulation outer proteins). Like T3Es of phytopathogenic bacteria, rhizobial T3Es are translocated through a T3SS into plant cells, where they interact with host components (Fauvart and Michiels, 2008; Schechter *et al.*, 2010; Wenzel *et al.*, 2010; Kimbrel *et al.*, 2013; Staehelin and Krishnan, 2015). NopM of *Sinorhizobium* (*Ensifer*) sp. NGR234, for example, is an E3 ubiquitin ligase that hijacks the eukaryotic ubiquitin system and probably labels host proteins for proteasome-dependent degradation (Xin *et al.*, 2012). To the benefit of rhizobia, T3Es can suppress plant defense reactions and stimulate nodulation signaling (Bartsev *et al.*, 2004; Zhang *et al.*, 2011; Xin *et al.*, 2012; Okazaki *et al.*, 2013; Jiménez-Guerrero *et al.*, 2015). On the other hand, negative effects of rhizobial T3Es on nodulation have been reported for certain strain–host combinations. Such T3E-triggered nodulation blockage can depend on host plant-specific R-proteins as shown recently for soybean genotypes carrying *Rj2* or *Rfg1* alleles (Yang *et al.*, 2010). Accordingly, T3SS mutants deficient in secretion of T3Es can nodulate various legumes that are incompatible with the wild-type strain (e.g. Meinhardt *et al.*, 1993; Viprey *et al.*, 1998; Okazaki *et al.*, 2009; Tsukui *et al.*, 2013; Staehelin and Krishnan, 2015). Mutants of *Sinorhizobium* sp. NGR234 lacking the protease NopT (belonging to the YopT/AvrPphB effector family) show improved nodulation properties on certain legumes (Dai *et al.*, 2008; Kambara *et al.*, 2009). When expressed in tobacco (*Nicotiana tabacum*) leaves, proteolytically active NopT proteins induce a rapid HR, suggesting R-protein mediated defense responses in this non-host plant (Dai *et al.*, 2008; Fotiadis *et al.*, 2012).

Sequences encoding NopL proteins are present in genomes of certain rhizobia but not in those of phytopathogenic bacteria (Supplementary Fig. S1 at *JXB* online). NopL of *Sinorhizobium* sp. NGR234 (locus NGR_a00770; formerly y4xL) is the prototype of this unique T3E family. Besides an N-terminal secretion signal sequence, NopL of NGR234 consists of two large repeats and a C-terminal domain. A prediction of the protein structure of NopL by homology modeling is currently impossible due to the lack of homologous protein structures. Previous work with a *nopL* knock-out mutant of NGR234 (mutant NGRΩ*nopL*; Marie *et al.*, 2003) showed that NopL antagonizes nodule senescence in beans (*Phaseolus vulgaris* cv. Tendergreen) as determined by analysis of necrosis of infected nodule cells (Zhang *et al.*, 2011). Similar to the T3E NopP of NGR234 (Skorpil *et al.*, 2005), NopL was found to be phosphorylated by crude plant protein extracts *in vitro*. The addition of the MAP kinase kinase inhibitor PD98059 to the reaction mixture resulted in reduced phosphorylation of NopL, providing first clues that NopL phosphorylation is associated with MAP kinase signaling (Bartsev *et al.*, 2003; Bartsev *et al.*, 2004). Further work showed that NopL expressed in tobacco or yeast (*Saccharomyces cerevisiae*) is multiply phosphorylated. A ladder of at least nine spots representing different phosphoproteins was observed when NopL was expressed in yeast and analyzed by two-dimensional (2D) gel electrophoresis. Accordingly, four phosphoserine residues in NopL were identified by mass spectrometry (Zhang *et al.*, 2011). All characterized phosphorylation sites possess a conserved serine–proline motif (SP site; Supplementary Fig. S2), which is typical for phosphorylation sites in MAP kinase substrates (Ishihama and Yoshioka, 2012; Hoehenwarter *et al.*, 2013; Meng and Zhang, 2013). NopL expression in eukaryotic cells impaired the induction of MAP kinase-mediated responses. In yeast cells of the *MAT*a mating type, mating pheromone (α-factor) signaling was disrupted by expression of NopL (Zhang *et al.*, 2011). Activation of this MAP kinase pathway by α-factor inhibits cell growth by interfering with the initiation of DNA replication, resulting in arrest of cells in the G_1 phase of the cell cycle (Bücking-Throm *et al.*, 1973). In tobacco leaves, expression of NopL impaired cell death, which was induced by expression of the constitutively active MAP kinase $SIPK^{DD}$ (salicylic acid-induced protein kinase of tobacco with substitutions of Thr218 and Tyr220 to aspartate in the TXY motif of the activation loop; Zhang *et al.*, 2011). Moreover, expression of NopL in tobacco and the legume *Lotus japonicus* thwarts expression of pathogenesis-related (PR) proteins, such as class I chitinase and class I glucanase (Bartsev *et al.*, 2004). Class I chitinase (CHN50) is a well-characterized marker of SIPK signaling in tobacco. The transcription factor WRKY1, which is phosphorylated by SIPK, was shown to bind specifically to a W box in the promoter of *CHN50* (Menke *et al.*, 2005). Hence, it was concluded that NopL suppresses plant defense reactions by interfering with MAP kinase signaling or downstream events (Zhang *et al.*, 2011). However, the molecular mechanisms underlying NopL function have remained unclear.

In this work, we show that NopL is targeted to plant nuclei and interacts with SIPK. *In vitro* phosphorylation experiments with recombinant proteins expressed in *Escherichia coli* revealed that NopL is phosphorylated by SIPK. Nodulation

experiments with *P. vulgaris* and various NGR234 mutant strains indicate that serine to alanine substitutions in the serine–proline motifs of NopL negatively affect symbiotic effector activity.

Materials and methods

Strains, plasmids, and primers

Bacterial strains, *Saccharomyces cerevisiae* strains, and plasmids used in this study are listed in Supplementary Table S1. Plasmids were constructed according to standard methods, and PCR primers used are listed in Supplementary Table S2.

Expression of NopL in yeast and tobacco

NopL and variants were expressed in yeast W303-1A (*MAT*a) and W303-1B (*MAT*α) cells harboring the corresponding plasmid DNA in SC liquid medium supplemented with 2% (w/v) galactose according to the pYES2 user manual from Invitrogen (Thermo Fisher Scientific, Waltham, MA, USA). Harvested proteins were subjected to western blot analysis with anti-NopL antibodies. Cell growth inhibition tests with transformed W303-1B cells were performed as described previously (Zhang *et al.*, 2011).

The halo assay with mating pheromone (α-factor) was performed according to previous studies (Hoffman *et al.*, 2002; Xin *et al.*, 2012). Briefly, W303-1A cultures expressing NopL and variants were grown to stationary phase in SD/–Leu liquid medium with 2% (w/v) glucose. Pelleted cells were re-suspended in H_2O (5×10^5 cells ml^{-1}) and then spread on SD/–Leu solid medium (500 µl cells per plate). A filter disk impregnated with 10 µg of α-factor (Sigma-Aldrich, St. Louis, MO, USA; dissolved in 10 µl H_2O) was placed into the center of each plate. Sealed plates were incubated at 30 °C for 1 week and then photographed.

NopL and variants were also expressed in *S. cerevisiae* strain SY2227 (harboring plasmid pRS316-GAL-STE4; activation of the mating pheromone signaling pathway on galactose plates in the absence of α-factor) (Cole *et al.*, 1990). Cells containing appropriate plasmids were grown on SD/–Leu medium plates containing either 2% (w/v) galactose or glucose at 30 °C for 1 week and then photographed.

For expression of NopL and NopL(S12xA) in tobacco (*N. tabacum* cv. Xanthi) leaves, plasmids pPZP112, pPZP-*nopL*, and pPZP-*nopL*(S12xA) (Supplementary Table S1) were introduced into *Agrobacterium tumefaciens* strain AGL1 by electroporation. Leaf infiltration with bacterial suspensions was performed as described previously (Zhang *et al.*, 2011).

Subcellular localization of NopL in plant cells

DNA encoding NopL or NopL(S12xA) was cloned into the vectors pX-DR (Chen *et al.*, 2009) and pCAMBIA 1302 (Cambia, Brisbane, Australia), which both contain the *Cauliflower mosaic virus* (CaMV) 35S promoter sequence, resulting in expression vectors for red fluorescent protein (RFP)–NopL, RFP–NopL(S12xA), NopL–green fluorescent protein (GFP), and NopL(S12xA)–GFP fusion proteins. Gold particles (1 µm in diameter; Bio-Rad, Hercules, CA, USA) were coated with plasmid DNA and then used for micro-projectile bombardment of epidermal onion cells with a Bio-Rad PDS-1000/He particle delivery system (1100 psi bombardment pressure; helium vacuum of 27 inHg; a distance of 12 cm to the sample). Bombarded onion cells were cultured on Murashige and Skoog medium (4.4 g l^{-1}; pH 5.8), supplemented with 39 g l^{-1} sucrose and 2.6 g l^{-1} phytagel (Sigma-Aldrich) at room temperature for 24 h. Cells were then examined with a confocal laser scanning microscope (TCS SP2; Leica, Wetzlar, Germany). For observation of either red or green fluorescence, the excitation wavelength of the laser beam was adjusted to either 561 nm or 488 nm. Where indicated, nuclei were stained with 4',6-diamidino-2-phenylindole (DAPI) and visualized using an excitation wavelength of 405 nm.

Bimolecular fluorescence complementation analysis

DNA encoding NopL or NopL(S12xA) was inserted into the vectors pSAT1-nEYFP-N1 and pSAT1-cEYFP-N1 (Citovsky *et al.*, 2006), which contain either N-terminal (nEYFP) or C-terminal (cEYFP) halves of enhanced yellow fluorescent protein (EYFP). The MAP kinase gene *SIPK* of tobacco (accession no. U94192) was cloned into pSAT1-cEYFP-N1. Onion epidermal cells were transformed by particle bombardment with the constructed plasmids as described above. Each pair of plasmids was used for bombardment in random order. Corresponding control plasmids were used before or after bombardment of the test sample to ensure that DNA was transferred under the same conditions (identical transformation efficiencies in a given experiment). Where indicated, plasmid pairs were used at an equal molar ratio (Hollender and Liu, 2010). Similar results were obtained in three independent experiments. Cells were analyzed by confocal laser scanning microscopy 24 h after bombardment. The excitation wavelength of the laser beam was adjusted to 514 nm for observation of yellow fluorescence and to 405 nm for visualization of DAPI-stained nuclei.

Expression and purification of recombinant proteins in E. coli

NopL and NopL(S12xA) were expressed as glutathione *S*-transferase (GST) fusion or His_6-tagged proteins in *E. coli* BL21 (DE3). Similarly, SIPK of tobacco and $NtMEK2^{DD}$, a constitutively activated form of the upstream MAP kinase kinase NtMEK2 (accession no. AF325168) with T227D/S233D substitutions (Yang *et al.*, 2001; Zhang and Liu, 2001) were expressed in *E. coli* (GST–$NtMEK2^{DD}$, $NtMEK2^{DD}$-His_6, GST–SIPK and His_6-SIPK, respectively). Proteins were purified from sonicated cells under native conditions with glutathione agarose beads (Novagen, Madison, WI, USA) or with Ni-NTA magnetic agarose beads (Qiagen, Germantown, MD, USA) according to the supplier's recommendations. Elution fractions were concentrated with Amicon Microcon concentrators (Amicon Ultra-0.5 centrifugal concentrator, YM-10; Millipore, Bedford, MA, USA). The purified proteins were equilibrated with an appropriate buffer and then used for western blot analysis, pull-down assays, and phosphorylation reactions.

Western blot analysis and pull-down assay

Equal amounts of proteins were separated by SDS–PAGE and then transferred to a nitrocellulose membrane. Blotted proteins were visualized with Ponceau S. The membranes were first blocked in TBST [50 mM Tris-HCl, pH 7.5, 150 mM NaCl, and 0.05% (v/v) Tween-20] with 5% (w/v) non-fat dry milk, followed by incubation for 1 h with 2500-fold diluted anti-NopL (Zhang *et al.*, 2011), 2000-fold diluted anti-chitinase I (Shinshi *et al.*, 1987), 2000-fold diluted anti-glucanase I (Felix and Meins, 1985), or 4000-fold diluted anti-His_6 (Roche, Basel, Switzerland). Corresponding horseradish peroxidase-conjugated second antibodies were employed on blots, which were subsequently developed by 3,3'-diaminobenzidine according to the supplier's instructions (Boster, Wuhan, China). Where indicated, western blots were visualized by electrochemiluminescence (ECL, Amersham GE Healthcare, Little Chalfont, UK) and signals quantified with the Image J software (rsb.info.nih.gov/ij).

A pull-down assay was performed according to a previously described method (Lane *et al.*, 2006). Affinity-purified recombinant proteins [GST, GST–NopL, GST–NopL(S12xA] and His_6-SIPK] were quantified using the Bradford method (Bradford, 1976). GST–NopL (100 µg), GST–NopL(S12xA) (100 µg), or GST (43 µg) were incubated with His_6-SIPK (141 µg) in 100 µl of phosphate-buffered saline (PBS; 137 mM NaCl, 2.7 mM KCl, 10 mM Na_2HPO_4, adjusted with NaOH to pH 7.4) at 4 °C for 2 h. The reaction mixture was then adjusted to a volume of 1 ml by adding glutathione agarose beads

(in PBS). One hour later, beads were collected by centrifugation (100 *g* for 10 s) and washed 10 times with PBS to remove unbound His_6-SIPK. Beads were then mixed with 5× SDS loading buffer [250 mM Tris–HCl (pH 6.8), 10% (w/v) SDS, 50% (v/v) glycerol, 0.5% (w/v) bromophenol blue, 5% (v/v) 2-mercaptoethanol] and boiled for 5 min. Finally, protein samples were centrifuged and subjected to SDS–PAGE followed by western blot analysis with an anti-His_6 monoclonal antibody.

In vitro *phosphorylation assay*

For *in vitro* phosphorylation reactions, recombinant NopL variants [GST–NopL, His_6-NopL, GST–NopL(S12xA), and His_6-NopL(S12xA); 0.5 μg μl^{-1}], GST–NtMEK2^{DD}, or NtMEK2^{DD}-His_6 (0.25 μg μl^{-1}) and GST–SIPK or His_6-SIPK (0.25 μg μl^{-1}) were used. Proteins were incubated at 30 °C for 30 min in a reaction mixture (30 μl) containing phosphorylation buffer (20 mM HEPES-KOH, pH 7.6, 1 mM DTT, and 10 mM $MgCl_2$) and 50 μM ATP (Sigma-Aldrich). Where indicated, reactions were supplemented with 50 μCi ml^{-1} [γ-^{32}P]ATP (PE Inc., USA). Reactions were stopped with 2× SDS–PAGE sample buffer, and proteins were analyzed either by 2D gel electrophoresis as described (Zhang *et al.*, 2011) or by one-dimensional gel electrophoresis followed by western blot analysis with anti-NopL antibodies. Autoradiography was performed with a Typhoon 9410 variable Mode Imager (GE Amersham Biosciences, Piscataway, NJ, USA). Where indicated, gels were stained with CBB (Coomassie Brilliant Blue G-250).

*Construction of NGR*ΩnopL-nopL*(S12xA)*

An ΩSpe interposon excised from pHP45W (Prentki and Krisch, 1984) was cloned into the pBluescript derivative pBS-p*nopL-nopL*(S12xA) (Supplementary Table S1) at the unique *Bam*HI site (Fig. 5A). The whole insert was then excised with *Xba*I and cloned into the *Xba*I site of the suicide vector pJQ-*y4mN* (Supplementary Table S1), a derivative of pJQ200-mp18 (Quandt and Hynes, 1993) that also carries a 1.5 kb fragment containing *y4mN* of *Sinorhizobium* sp. NGR234 (locus NGR_a02450; a putative transketolase gene without symbiotic function). The constructed suicide plasmid was then mobilized into strain NGRΩ*nopL* (Marie *et al.*, 2003) by tri-parental mating (Figurski and Helinski, 1979). Clones resistant to rifampin and spectinomycin were selected. PCRs were performed with genomic DNA and primers 47 and 48 (Supplementary Table S2) to confirm insertion *in trans* of the p*nopL-nopL*(S12xA) sequence at the *y4mN* site.

*Construction of NGR*ΩnopL *carrying pFAJ1702 derivatives*

Derivatives of pBluescript II SK (+) containing the *nopL* promoter and different *nopL* sequences [encoding NopL, NopL(S4xA), NopL(S6xA), NopL(S8xA), NopL(S10xA), and NopL(S12xA), respectively; Supplementary Fig. S2] were constructed by various PCR and cloning procedures (Supplementary Table S1). The fragments were then inserted into the *Kpn*I and *Xba*I sites of pFAJ1702 (Dombrecht *et al.*, 2001), resulting in plasmids pFAJ-*nopL*, pFAJ-*nopL*(S4xA), pFAJ-*nopL*(S6xA), pFAJ-*nopL*(S8xA), pFAJ-*nopL*(S10xA), and pFAJ-*nopL*(S12xA). The plasmids were then mobilized into NGR234Ω*nopL* by tri-parental mating (Supplementary Table S1).

Analysis of secreted proteins

Proteins in culture supernatants from the strains NGRΩ*nopL*, NGR234 (wild type), NGRΩ*nopL-nopL*(S12xA), and NGRΩ*nopL* carrying different pFAJ1702 derivatives were subjected to western blot analysis with anti-NopL antibodies. Cultures were supplemented with 1 μM apigenin and then concentrated according to previously described procedures (Marie *et al.*, 2003; Hempel *et al.*, 2009; Xin *et al.*, 2012). Finally, secreted proteins were subjected to SDS–PAGE (gels stained with CBB) and western blot analysis.

Nodulation tests

Nodulation tests with *P. vulgaris* (cv. Tendergreen; Groves Nurseries, Bridport, Dorset, UK) were performed according to previously described procedures in sterilized 300-ml plastic jar units (e.g. Staehelin *et al.*, 2006). Plantlets (one plant per jar) were inoculated with a 2 ml suspension containing ~10^9 bacteria. Plants were grown at 24 ± 2 °C in an air-conditioned greenhouse with a 16/8 h light/dark cycle. Nodules were harvested at 45 d (Fig. 5C, D) or 52 d (Fig. 6B) post-rhizobial inoculation, cut into two parts, and photographed. Areas of central infected zones and dark (often necrotic) areas of senescent cells within these zones were quantified for each nodule half using the image processing software ImageJ (rsb.info.nih.gov/ij). Data were statistically analyzed using the Kruskal–Wallis rank sum test. A *P*-value of ≤0.01 was considered as significant. Where indicated, effects of strains secreting different NopL variants were compared by linear regression analysis.

Bioinformatic analysis

Putative phosphorylation sites of NopL were predicted by NetPhos 2.0 Server (http://www.cbs.dtu.dk/services/NetPhos/) or Plantphos software (http://csb.cse.yzu.edu.tw/PlantPhos/). For phylogenic analysis, the amino acid sequence of NopL from *Sinorhizobium* sp. NGR234 (accession no. NP_444148) was used as a query sequence for protein blast (blastp algorithm) or nucleotide blast (blastn algorithm) searches at the NCBI homepage (http://www.ncbi.nlm.nih.gov/) using non-redundant (nr) protein and nucleotide databases as well as the 'wgs' (whole-genome shotgun) nucleotide database. All DNA sequences were translated into protein sequences. A phylogenetic tree with in total 17 obtained rhizobial NopL sequences (see Supplementary Fig. S1) was constructed with the MEGA 5 program using the Neighbor–Joining method (Tamura *et al.*, 2011). The Poisson correction method was applied for evolutionary distances. The PredictProtein server (Rost *et al.*, 2004) was used to search for prediction of disordered regions in the NopL sequence.

Results

Serine residues in NopL are required for effector activity in yeast and tobacco

When expressed in yeast, NopL is multiply phosphorylated and inhibits mating pheromone (α-factor) signaling (Zhang *et al.*, 2011). Previously identified phosphoserine residues (serine–proline motifs in both tandem repeats of NopL) are shown in Supplementary Fig. S2. To test the importance of serine residues for effector activity in yeast, we constructed plasmids (pBluescript II derivatives) encoding NopL variants with serine to alanine substitutions. The protein NopL(S4xA) contains substitutions at the four identified phosphorylation sites. Furthermore, plasmids encoding NopL(S12xA) and NopL(S14xA) with 12 and 14 serine to alanine substitutions were constructed. These NopL forms are based on NopL(S4xA). They possess additional serine to alanine substitutions in the serine–proline motifs of NopL and in a GPSHSGPSQARPSH motif at the end of the second tandem repeat previously suggested to be important for effector function (Zhang *et al.*, 2011). The constructs were cloned into the vector pESC-leu, which allows protein expression in yeast under the control of a galactose-inducible promoter (GAL1).

Expression of the NopL variants in transformed W303-1A (*MAT*a) yeast cells was verified by western blot analysis with anti-NopL antibodies. Bands corresponding to the predicted size of NopL (37 kDa) were observed, while the sample from control cells transformed with the empty vector pESC-leu lacked this band (Fig. 1A). Yeast cells expressing NopL on galactose plates failed to produce a clear halo around a filter paper disk containing the mating pheromone (α-factor), indicating that NopL compromised α-factor-induced MAP kinase signaling as reported previously (Zhang *et al.*, 2011). In contrast, cells expressing NopL(S12xA) or NopL(S14xA) showed distinct halos, which were comparable with those of control cells transformed with pESC-leu. A faint halo of intermediate size was observed for NopL(S4xA)-expressing yeast cells (Fig. 1B).

To substantiate these findings, we also transformed yeast strain SY2227 with the constructed plasmids. SY2227 is a modified strain, in which the α-factor signaling pathway is activated by overexpression of STE4 by galactose. SY2227 therefore does not show any growth on galactose plates (Cole *et al.*, 1990). In contrast to cells transformed with pESC-leu, SY2227 cells expressing NopL grew on SD medium containing galactose, indicating that NopL could inhibit STE4-induced α-factor signaling in SY2227. In contrast to NopL, expression of NopL(S12xA) or NopL(S14xA) in SY2227 did not promote cell growth of STE4-overexpressing cells. SY2227 cells expressing NopL(S4xA) grew slowly on SD/galactose plates, which is related to the intermediate phenotype observed for the halo assay with α-factor (Fig. 1C).

Furthermore, we used a previously established growth inhibition assay to test cytostatic effects in yeast strain W303-1B (*MAT*α) (Zhang *et al.*, 2011). In contrast to NopL, expression of NopL(S12xA) in this strain did not show any effect on cell growth (Supplementary Fig. S3).

Finally, we compared the effects of NopL and NopL(S4xA) transiently expressed in plant cells. Under the conditions used, tobacco leaves infiltrated with *A. tumefaciens* show activated MAP kinase signaling and subsequent expression

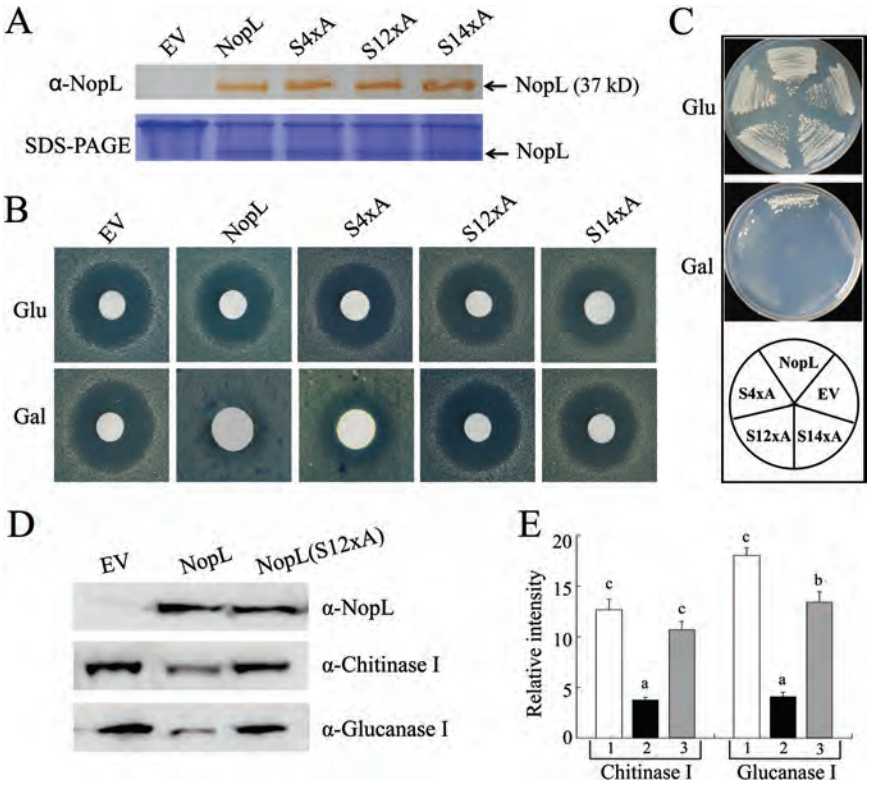

Fig. 1. Effects of NopL variants on α-factor-induced MAP kinase signaling in yeast (A–C) and on accumulation of PR proteins in tobacco (D and E). The NopL variants NopL(S4xA), NopL(S12xA), and NopL(S14xA) in A-C are shortened to S4xA, S12xA, and S14xA. (A) Western blot analysis of NopL and the indicated variants expressed in yeast strain W303-1A. Proteins from cells transformed with the empty vector pESC-leu (lane EV) were included as a control. Extracted proteins (1 μg) were probed using anti-NopL antibodies (α-NopL). An SDS–PAGE gel stained with Coomassie Brilliant Blue G-250 (CBB) indicated equal amounts of loaded proteins. (B) Halo assay with α-factor on SD medium agar plates with 2% (w/v) glucose (Glu) or 2% (w/v) galactose (Gal). W303-1A cells expressing NopL and the indicated variants on galactose plates and W303-1A cells transformed with the empty vector pESC-leu (EV) were used for the assay. A paper filter disk impregnated with 10 μg of α-factor was added to the center of the plate, and photographs were taken 1 week later. (C) Growth of yeast strain SY2227 derivatives expressing NopL or the indicated variants on SD/galactose. Cells were spread on SD medium plates supplemented with either 2% (w/v) glucose (Glu) or galactose (Gal) without leucine. Photographs were taken 1 week after inoculation. (D) Western blot analysis of PR proteins in tobacco leaves expressing NopL or NopL(S12xA). Leaves infiltrated with *A. tumefaciens* carrying the empty binary vector (EV) were used for comparison. Plant material was harvested 3 d post-infiltration and probed with antisera against NopL, class I chitinase, and class I glucanase. The proteins were visualized by electrochemiluminescence. The shown western blots represent examples. (E) Quantification of the PR protein expression data with Image J software [EV, column 1; NopL expression, column 2; NopL(S12xA) expression, column 3]. Data (relative intensities) indicate means ±SE from five independent transformation events (n=5). Different letters indicate significant differences (Kruskal–Wallis test; $P \leq 0.01$).

of PR proteins. Western blot analysis indicated that NopL expression significantly suppressed accumulation of PR proteins. In contrast, NopL(S12xA) expression had no effect on production of class I chitinase and only slightly influenced the levels of class I β-1,3-glucanase (Fig. 1D, E). Taken together, our data show that NopL and NopL(S12xA) differ in effector activity as analyzed in various biological test systems.

NopL is targeted to the plant nucleus

To study the subcellular localization of NopL and NopL(S12xA) within plant cells, the proteins fused to fluorescent tags were expressed in onion (*Allium cepa* L.). Onion epidermal cells were used because of their suitability for microscopic analysis and their transformability by DNA bombardment with a particle delivery system, which enables rapid and synchronous transformation. RFP was fused to the N-termini [RFP–NopL and RFP–NopL(S12xA) proteins] and GFP to the C-termini [NopL–GFP and NopL(S12xA)–GFP proteins]. Cells expressing the corresponding fusion proteins were photographed 24 h after particle bombardment. As expected, RFP and GFP control proteins could be detected in the cytoplasma, plasma membranes, and nuclei. In cells expressing the NopL and NopL(S12xA) fusion proteins, fluorescence predominantly appeared in the nuclei (Fig. 2A, B). These observations show that all four fluorescent NopL proteins can be targeted to the nucleus regardless of whether the fluorescent tags are fused to the N- or C-terminal ends of the protein.

NopL interacts with the MAP kinase SIPK

Previous work showed that NopL inhibited cell death induced by overexpression of the MAP kinase SIPK in tobacco, indicating that NopL targets SIPK or disrupts downstream elements of MAP kinase signaling (Zhang *et al.*, 2011). Elicitor-treated tobacco cells accumulate activated SIPK protein in their nuclei (Dahan *et al.*, 2009). To test whether NopL physically interacts with SIPK, we used a bimolecular fluorescence complementation (BiFC) approach. Plasmids were constructed which contain the CaMV 35S promoter and DNA encoding proteins fused to EYFP fragments (nEYFP and cEYFP, respectively). The fusion proteins, namely NopL–nEYFP, NopL(S12xA)–nEYFP, and SIPK–cEYFP, as well as the nEYFP and cEYFP fragments alone, were then expressed in onion cells after particle bombardment. As shown in Fig. 3, yellow fluorescence emission reflecting formation of a BiFC complex was seen in nuclei for the combination of NopL–nEYFP and SIPK–cEYFP. No fluorescence complementation was seen, however, for control combinations such as NopL–nEYFP with cEYFP or nEYFP with SIPK–cEYFP. Notably, fluorescent nuclei were not observed for the combination NopL(S12xA)–nEYFP with SIPK–cEYFP. These data indicate that NopL, but not NopL(S12xA), physically interacts with SIPK in nuclei.

A pull-down assay with purified recombinant proteins expressed in *E. coli* was performed to provide further evidence for physical interaction between NopL and SIPK. As shown in Supplementary Fig. S4, GST–NopL was able partially to pull down His_6-SIPK, whereas the use of GST alone and GST–NopL(S12xA) resulted in faint background signals (Supplementary Fig. S4).

NopL is a MAP kinase substrate

As NopL interacts with SIPK, we asked whether NopL can be phosphorylated by SIPK. We used [γ-^{32}P]ATP to demonstrate incorporation of ^{32}P into His_6-NopL. Recombinant proteins expressed in *E. coli* were used for the *in vitro* phosphorylation assay. His-tagged SIPK was activated by the GST-tagged MAP kinase kinase $MEK2^{DD}$, which is constitutively active (Yang *et al.*, 2001). As shown in Fig. 4A, phosphorylated His_6-NopL was clearly detected by autoradiography, whereas a corresponding reaction with His_6-NopL(S12xA) did not

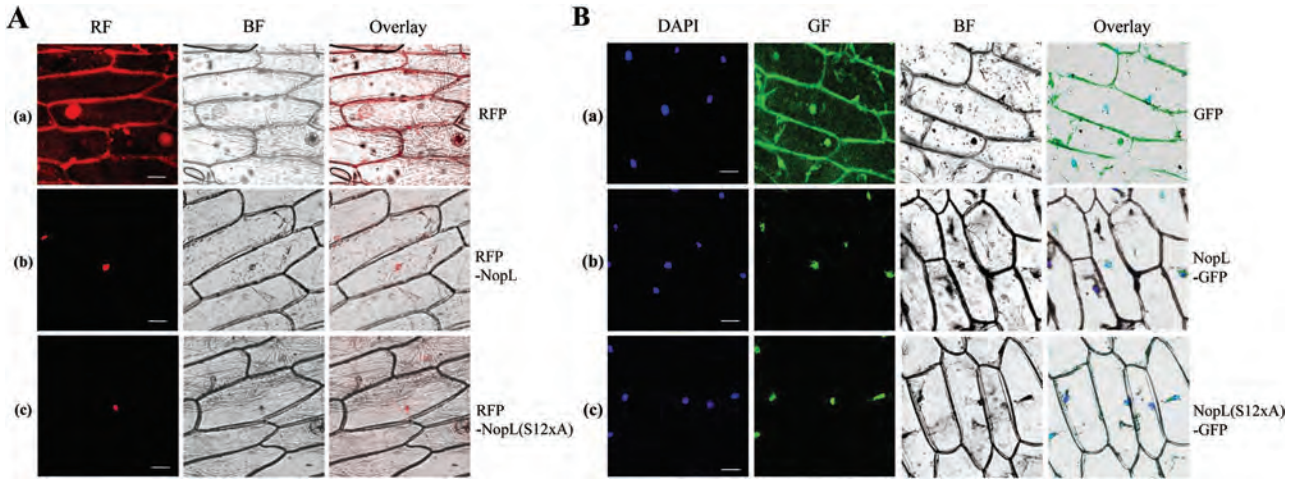

Fig. 2. NopL is targeted to the nucleus. NopL and NopL(S12xA) proteins with fluorescent protein tags were expressed in epidermal onion cells and visualized by confocal microscopy to determine their subcellular localization. (A) Subcellular localization analysis of RFP–NopL, RFP–NopL(S12xA), and RFP alone (control). Cells were analyzed for red fluorescence (RF) emission and under bright field (BF) illumination 24 h after particle bombardment. Scale bars=200 μm. (B) Subcellular localization analysis of NopL–GFP and NopL(S12xA)–GFP. Cells were analyzed for green fluorescence (GF) emission and under BF illumination 24 h after particle bombardment. Nuclei were stained with 4',6-diamidino-2-phenylindole (DAPI). Scale bars=200 μm.

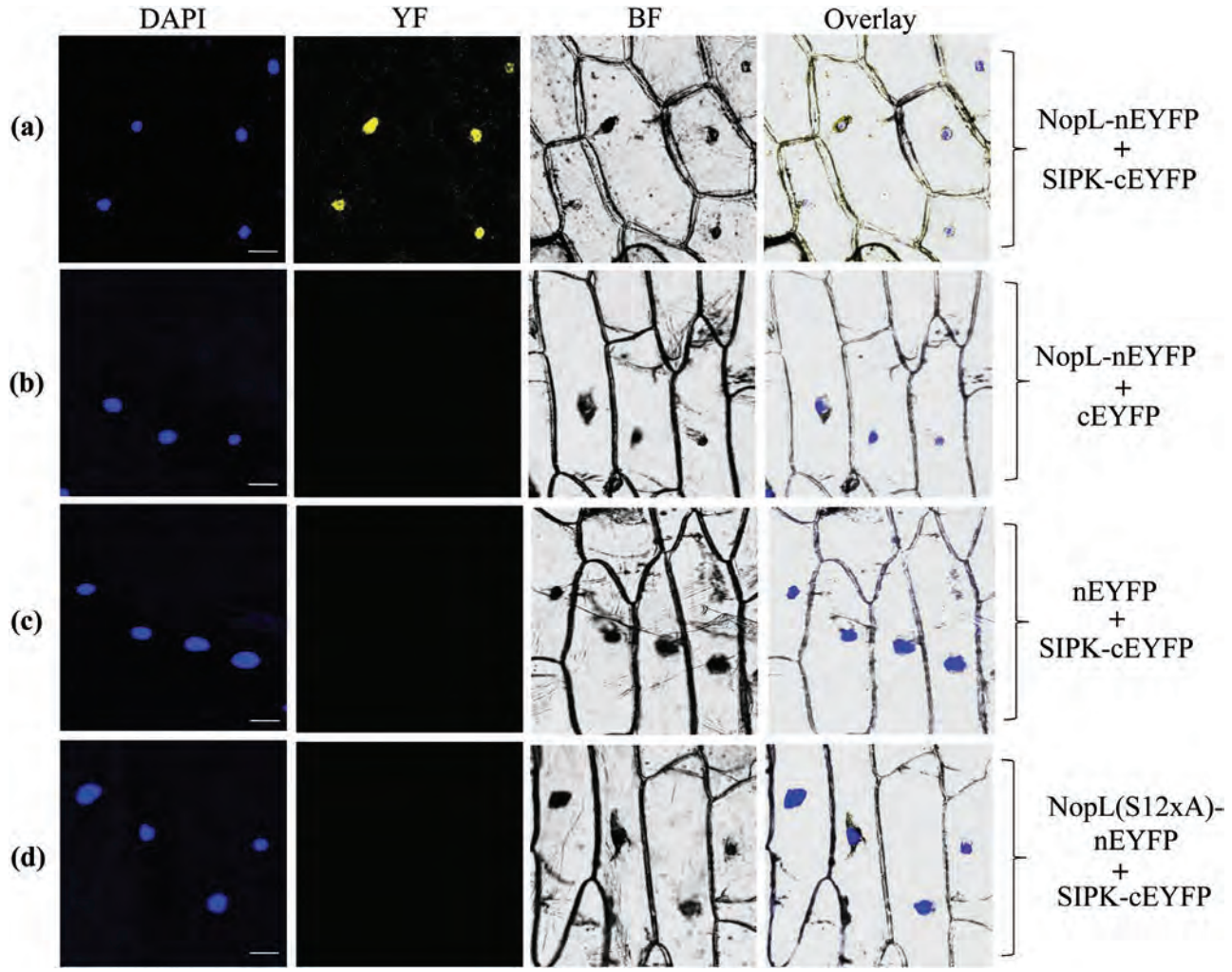

Fig. 3. NopL interacts with SIPK in the nucleus. BiFC analysis was performed with onion cells expressing the indicated protein combinations. Representative confocal micrographs were taken 24 h after particle bombardment. cEYFP and nEYFP alone were used as controls. Cells were analyzed for yellow fluorescence (YF) emission and under bright field (BF) illumination. Only the combination NopL–nEYFP with SIPK–cEYFP resulted in formation of a BiFC complex. Nuclei were stained with DAPI. Scale bars=200 μm.

result in any visible signal. SDS–PAGE and western blot analysis with anti-NopL antibodies showed that phosphorylated His_6-NopL forms migrated more slowly on the gel.

Furthermore, GST-tagged NopL variants [GST–NopL and GST–NopL(S12xA)] were analyzed after 2D gel electrophoresis. In this assay, His_6-SIPK was activated by $MEK2^{DD}$-His_6. After completion of the phosphorylation reaction, GST–NopL or GST–NopL(S12xA) were purified with glutathione agarose beads and then subjected to 2D gel electrophoresis followed by immune staining with anti-NopL antibodies. GST–NopL phosphorylated by His_6-SIPK was separated into at least nine distinct spots, indicating that NopL was multiply phosphorylated (Fig. 4B). These spots were not observed for a corresponding control lacking His_6-SIPK (Fig. 4C). When GST–NopL(S12xA) was used for the phosphorylation assay, only faint background signals were seen (Fig. 4D).

Nodulation tests

To investigate the importance of serine residues in NopL for symbiotic effector activity, we examined the effects of different NopL variants in nodules of *P. vulgaris* (cv. Tendergreen). Previous nodulation experiments with *Sinorhizobium* sp. NGR234 and the knock-out mutant NGRΩ*nopL* showed that NopL can antagonize nodule senescence of this host plant (Zhang *et al.*, 2011). We first constructed an NGR234 derivative that expresses NopL(S12xA) instead of NopL. In this mutant, named NGRΩ*nopL-nopL*(S12xA), the coding sequence for NopL(S12xA) with the upstream *nopL* promoter is stably inserted into the *y4mN* site of NGRΩ*nopL* (Fig. 5A). The parent strain NGRΩ*nopL* and the wild-type strain NGR234 were included in the experiments. The NopL(S12xA) of strain NGRΩ*nopL-nopL*(S12xA) and NopL of NGR234 were detected by western blot analysis in supernatants of flavonoid-induced cultures, indicating equal expression and protein secretion through the T3SS (Fig. 5B). The three strains were then used to inoculate *P. vulgaris* (cv. Tendergreen) seedlings. Nodules harvested 45 d post-inoculation were cut into two halves and photographed (Fig. 5C). The area of senescent cells in the central infected zone of a given nodule was quantified with the image processing software ImageJ and then expressed as a percentage

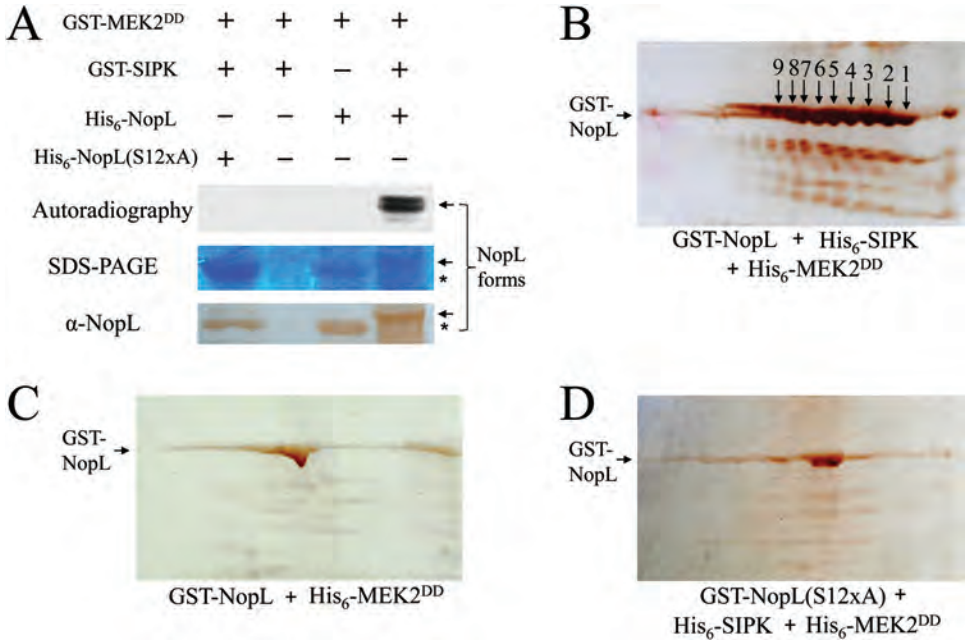

Fig. 4. NopL is phosphorylated by SIPK *in vitro*. Recombinant proteins were expressed in *E. coli* BL21 (DE3), purified by affinity chromatography, and used for phosphorylation assays. (A) Incorporation of ^{32}P into His_6-NopL by GST–SIPK. His_6-NopL or His_6-NopL(S12xA), GST–SIPK, and GST–$MEK2^{DD}$ proteins were incubated in phosphorylation buffer supplemented with [γ-^{32}P]ATP. The reaction mixture was separated by SDS–PAGE, stained with CBB, and subjected to autoradiography. Western blot analysis with anti-NopL antibodies confirmed that the observed autoradiography signal corresponds to His_6-NopL. Phosphorylated and non-phosphorylated NopL forms are marked with arrows and asterisks, respectively. (B–D) Western blot analysis with anti-NopL antibodies after 2D gel electrophoresis. The indicated proteins were used for the phosphorylation reaction. Phosphorylated GST–NopL (mol. wt ~70 kDa) was separated into at least nine protein spots.

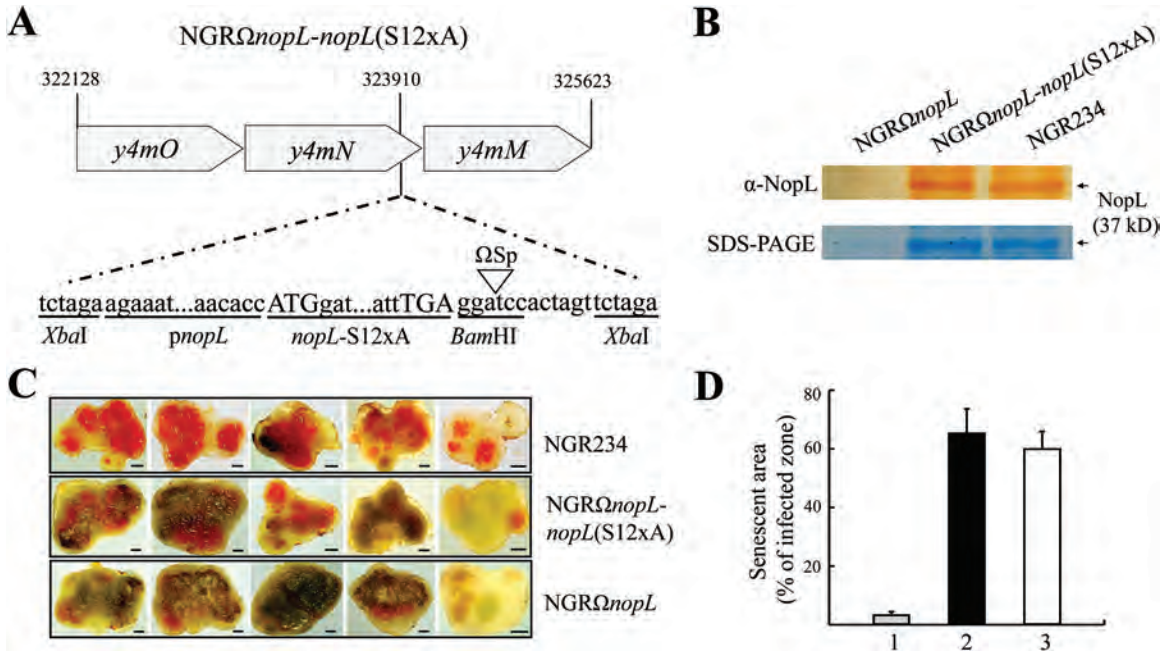

Fig. 5. *Phaseolus vulgaris* nodules induced by the mutant strains NGRΩ*nopL* and NGRΩ*nopL*-*nopL*(S12xA) show premature nodule senescence to a similar degree. (A) Schematic representation of the NGRΩ*nopL*-*nopL*(S12xA) mutant of *Sinorhizobium* sp. strain NGR234. The mutant is a NGRΩ*nopL* derivative with a 3 kb insertion *in trans* at the *Xba*I site of *y4mN* (locus NGR_a02450). The inserted sequence consists of the *nopL* promoter, the *nopL* coding sequence, and a spectinomycin Ω interposon (Ωsp) at the indicated *Bam*HI site. (B) Western blot analysis of secreted NopL and NopL(S12xA). Proteins from culture supernatants of the indicated strains were separated by SDS–PAGE (gels stained by CBB) and probed with anti-NopL antibodies. (C) Representative nodules of *P. vulgaris* cv. Tendergreen induced by the indicated strains at the time of harvest (45 d post-inoculation). Scale bars=1 mm. (D) Percentage of the senescence area from nodules induced by *Sinorhizobium* sp. NGR234 (column 1), NGRΩ*nopL* (column 2), and NGRΩ*nopL*-*nopL*(S12xA) (column 3) on the host plant *P. vulgaris* cv. Tendergreen. Areas of senescence (relative units) in infected zones were quantified by image analysis with ImageJ software. Data indicate means ±SE from at least 23 photographed nodule halves.

of the total area of the infected zone (Fig. 5D). Senescence in nodules induced by NGRΩ*nopL-nopL*(S12xA) was similar to that of NGRΩ*nopL* (Kruskal–Wallis test; P=0.317). The NopL-expressing wild-type strain NGR234, however, showed significantly reduced senescence as compared with NGRΩ*nopL-nopL*(S12xA) or NGRΩ*nopL* (P<0.001). Hence, NopL(S12xA) lacks the ability to antagonize nodule senescence.

A slightly modified test system was used to examine the symbiotic activity of NopL variants with different numbers of serine to alanine substitutions in the serine–proline motifs, namely NopL(S4xA), NopL(S6xA), NopL(S8xA), and NopL(S10xA) (Supplementary Fig. S2). Differently mutated *nopL* gene constructs, including the *nopL* promoter sequence, were inserted into pFAJ1702, an RK2-derived plasmid with improved stability properties (Dombrecht *et al.*, 2001). NGRΩ*nopL* strains harboring the constructed plasmids secreted all tested NopL variants equally, as analyzed by western blot analysis (Fig. 6A). The strains were then used in the nodule senescence test on *P. vulgaris* as before (Fig. 6B). NopL(S4xA) showed senescence-suppressing activity comparable with the non-modified NopL protein. Decreased effector activity was found for NopL(S6xA) and NopL(S8xA) with two and four additional serine to alanine substitutions at predicted phosphorylation sites. The strain secreting NopL(S10xA) with 10 substituted serine residues induced strong nodule senescence, comparable with the control strains secreting NopL(S12xA) or no NopL (empty vector pFAJ1702). Hence, the symbiotic activity of NopL(S10xA) was completely abolished. Based on data presented in Fig. 6B, linear regression analysis revealed that an increasing number of substituted serine residues in serine–proline motifs correlates with progressive loss of activity from NopL(S4xA) to NopL(S10xA) (R^2=0.9747).

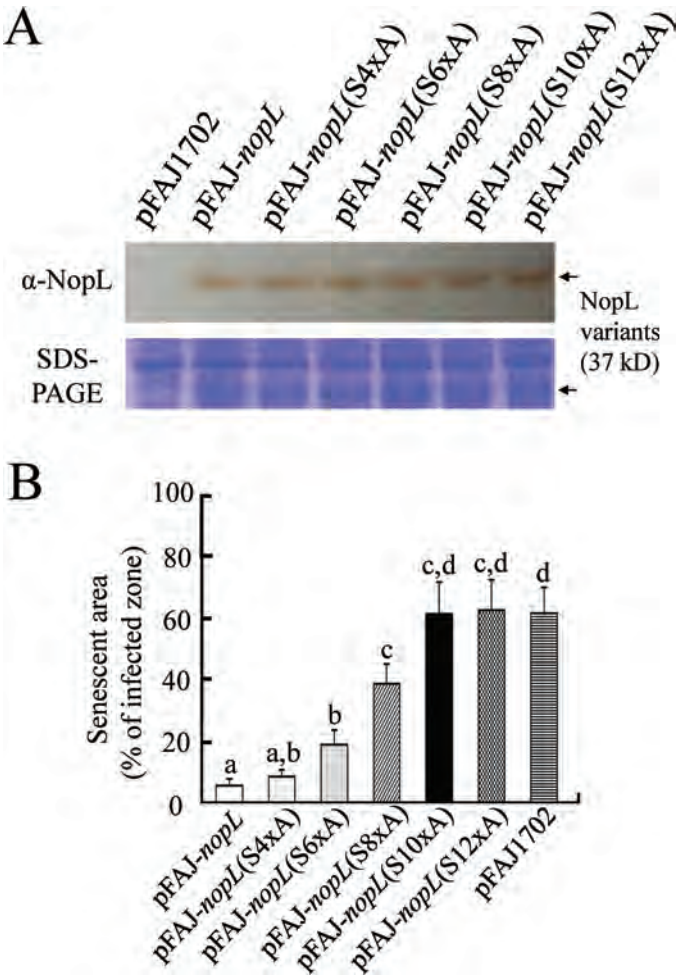

Fig. 6. Symbiotic characterization of NGRΩ*nopL* derivatives secreting NopL variants with serine to alanine substitutions. NGRΩ*nopL* harboring the indicated plasmids (pFAJ1702 derivatives) were constructed that secrete NopL, NopL(S4xA), NopL(S6xA), NopL(S8xA), NopL(S10xA), and NopL(S12xA) (names of strains were abbreviated to the names of the plasmids that they carried, e.g. NGRΩ*nopL* pFAJ-*nopL* was shortened to pFAJ-*nopL*). (A) Western blot analysis of secreted NopL and NopL variants. Proteins from culture supernatants of the indicated strains were separated by SDS–PAGE (gels stained by CBB) and probed with anti-NopL antibodies. (B) Percentage of the senescence area from *P. vulgaris* cv. Tendergreen nodules induced by NGRΩ*nopL* pFAJ-*nopL*, NGRΩ*nopL* pFAJ-*nopL*(S4xA), NGRΩ*nopL* pFAJ-*nopL*(S6xA), NGRΩ*nopL* pFAJ-*nopL*(S8xA), NGRΩ*nopL* pFAJ-*nopL*(S10xA), NGRΩ*nopL* pFAJ-*nopL*(S12xA), and NGRΩ*nopL* pFAJ1702. Areas of senescence (relative units) in infected zones were quantified by ImageJ image analysis. Data indicate means ±SE from at least 20 photographed nodule halves. Different letters indicate differences (Kruskal–Wallis test; $P \leq 0.05$).

Discussion

T3Es of virulent bacteria can target MAP kinase signaling in host cells, in order to suppress defense responses against the invading pathogen. For example, T3Es that possess phosphothreonine lyase activity, such as OspF of *Shigella flexneri* and HopAI1 of *Pseudomonas syringae*, irreversibly dephosphorylate and thus inactivate MAP kinases in host cells (Li *et al.*, 2007; Zhang *et al.*, 2007). Once delivered to *Arabidopsis thaliana* cells, the T3E AvrB of *P. syringae* interacts with and promotes phosphorylation of MAP kinase 4, resulting in perturbation of hormone signaling and enhanced plant susceptibility (Cui *et al.*, 2010). The T3Es YopJ of *Yersinia pestis*, VopA of *Vibrio parahemeolyticus*, as well as AvrA of *Salmonella typhimurium* are acetyltransferases that acetylate and thereby inactivate mammalian MAP kinase kinases (Mukherjee *et al.*, 2006; Trosky *et al.*, 2007; Jones *et al.*, 2008). Furthermore, HopF2 of *P. syringae* interacts with a MAP kinase kinase of *A. thaliana* and blocks kinase activity by ADP-ribosylation of the target protein (Wang *et al.*, 2010). Here we show that NopL of *Sinorhizobium* sp. NGR234 is a MAP kinase substrate. We found that NopL forms a complex with the MAP kinase SIPK and that NopL is phosphorylated by SIPK. As NopL is hyperphosphorylated *in vitro* (Fig. 4) and *in vivo* (Zhang *et al.*, 2011), interactions between NopL and MAP kinases seem to be reversible and variable, because each phosphorylated serine residue in NopL reflects another combination of the steric interaction between NopL and the catalytic center of the MAP kinase. The phosphorylation site motifs in NopL are perhaps sufficient for the formation of protein complexes with MAP kinases as we did not identify any additional putative MAP kinase docking site motifs (Tanoue *et al.*, 2000; Sharrocks *et al.*, 2000) in the NopL sequence.

NopL is predicted to contain various disordered regions (PredictProtein; Rost *et al.*, 2004) and apparently possesses a high degree of structural plasticity, which may facilitate interaction with a broad range of structurally conserved MAP kinases. The NopL–SIPK complex can therefore be regarded as representative for interactions between NopL and MAP kinases in general. As NopL expressed in yeast blocks mating pheromone signaling, it is likely that NopL also interacts with the MAP kinase FUS3 (Hilioti *et al.*, 2008). We suggest that NopL has the ability to interact with MAP kinases in various eukaryotic cells and thus may inspire medical researchers to test its possible pharmaceutical potential.

Remarkably, most of the verified or predicted phosphorylation sites are localized in the repeat region of NopL (Supplementary Fig. S2). Similar motifs are also conserved in NopL sequences of other rhizobial strains (Supplementary Fig. S1). During evolution, duplications of MAP kinase phosphorylation motifs appear to have taken place in *nopL* genes. Protein variants with more hyperphosphorylated repeats may possess increased affinity for MAP kinases.

As T3Es often irreversibly inactivate their host targets, it is tempting to speculate that NopL is a MAP kinase-inactivating enzyme. However, our phosphorylation experiments indicate that NopL was multiply phosphorylated by SIPK, providing evidence that SIPK was enzymatically active (Fig. 4). NopL was used at a higher concentration than SIPK in the phosphorylation test, and thus a single SIPK molecule repeatedly formed a protein complex with NopL. It is therefore unlikely that NopL irreversibly inactivates SIPK after formation of a NopL–SIPK complex.

The findings of this study indicate that NopL is a nuclear MAP kinase substrate, providing certain molecular explanations for the observed inhibitory effect of NopL on MAP kinase-regulated defense gene activation in plant cells (Fig. 1; Bartsev *et al.*, 2004). One possible explanation would be that NopL competitively inhibits phosphorylation of various natural substrates of MAP kinases such as WRKY transcription factors, which are known to regulate expression of genes encoding PR proteins including tobacco class I chitinase (Menke *et al.*, 2005; Ishihama *et al.*, 2012; Meng and Zhang, 2013). In fact, certain motifs in the repeat region of NopL show weak amino acid sequence similarities with a predicted WRKY transcription factor of soybean (accession no. XP_003528613; BlastP program; E-value: 5e-04), suggesting that NopL mimics a MAP kinase substrate.

Our subcellular localization analysis of fluorescent fusion proteins provides evidence that NopL is predominantly localized in nuclei of plant cells. Since NopL forms carrying either N- or C-terminal fluorescent tags are targeted to nuclei, free termini in NopL are obviously not required for nuclear localization (Fig. 2). Similar to other T3Es (Hicks and Galán, 2013), we did not identify any recognizable nuclear localization signal (Marfori *et al.*, 2011) and thus the mechanisms for nuclear import of NopL remain to be elucidated. Interestingly, NopL(S12xA) seems to enter the nucleus in a similar way to NopL. Formation of a NopL–MAP kinase complex is obviously not necessary for nuclear targeting. We suggest that NopL is first delivered to the host nucleus by interacting with another host protein. Once it has entered the nucleus, NopL would adopt the strategy to interact with nuclear MAP kinases.

The effect of NopL in prolonging the lifespan of infected cells in *P. vulgaris* nodules (Figs 5, 6; Zhang *et al.*, 2011) together with our findings that NopL is a MAP kinase substrate suggest that formation of the observed necrotic lesions in nodules depends on MAP kinase signaling. In fact, the cell death suppression activity of NopL in *P. vulgaris* nodules is reminiscent of the suppressive effect of NopL on cell death of tobacco cells induced by SIPK overexpression (Zhang *et al.*, 2011). We suggest that the observed necrotic spots in *P. vulgaris* nodules are the result of an apoptosis-like HR that is regulated by MAP kinase signaling and elicited by oxidative stress (Puppo *et al.*, 2005) or incompatible rhizobia. In contrast to expression in yeast (Fig. 1B, C), NopL(S4xA) retained full effector activity in the nodule senescence test. Compared with non-modified NopL, NopL(S6xA) and NopL(S8xA) showed significantly reduced symbiotic effector activity, whereas NopL(S10xA) was inactive (Fig. 6B). In other words, the loss of serine–proline motifs in NopL progressively reduced the symbiotic activity of NopL in *P. vulgaris* nodules. The serine to alanine substitutions in NopL could influence effector activity in different ways. For example, translocation of NopL from bacteria to host cells could be altered in NopL variants with an altered N-terminal sequence (Supplementary Fig. S2). However, secretion of the tested protein variants through the T3SSs was not altered (Fig. 6B). Although it cannot be excluded that the serine to alanine substitutions performed cause structural changes of NopL independently of phosphorylation, our results provide support for a close relationship between effector activity and phosphorylation. Effector activation processes via phosphorylation by host kinases have been shown or proposed for various T3Es of *P. syringae* (Anderson *et al.*, 2006; Desveaux *et al.*, 2007; Xiao *et al.*, 2007; Yeam *et al.*, 2010; Giska *et al.*, 2013) as well as for tyrosine-phosphorylated T3Es such as Tir of enteropathogenic *E. coli* and Tarp of *Chlamydia trachomatis* (Hayashi *et al.*, 2013).

Taken together, we show in this study that NopL interacts with MAP kinases and becomes hyperphosphorylated. Unphosphorylated NopL probably possesses the highest affinity for MAP kinases, and hyperphosphorylated NopL may no longer function as a MAP kinase interactor. Future work is needed to test whether phosphorylated NopL forms can be recycled by a host phosphatase activity and whether hyperphosphorylated NopL targets host components different from MAP kinases.

Supplementary data

Supplementary data are available at *JXB* online.

Figure S1. Phylogenic tree of the NopL effector family.

Figure S2. Serine-to-alanine substitutions in NopL analyzed in this study.

Figure S3. Expression of NopL and NopL(S12xA) in yeast strain W303-1B.

Figure S4. Pull-down assay.
Table S1. Plasmids and strains used in this work.
Table S2. Primers used in this study.

Acknowledgements

We are grateful to Frederick Meins (Friedrich Miescher Institute, Basel, Switzerland) for providing antibodies against chitinase and β-1,3-glucanase of tobacco. We thank Guo-Liang Wang (Hunan Agricultural University, Changsha, China) for providing pX-DR, Shuqun Zhang (University of Missouri, Columbia, MO, USA) for SIPK cDNA, Jan Michiels (Katholieke Universiteit Leuven, Belgium) for pFAJ1702, and William J. Broughton (University of Geneva, Switzerland) for NGRΩ*nopL*, pPZP-*nopL*, and pPROEX-*nopL*. Ming-Ting Liang (Sun Yat-sen University) is acknowledged for construction of pJQ-y4mN. This study was supported by the National Basic Research Program of China (973 program, no. 2010CB126501), by the National Natural Science Foundation of China (grants 31270128 and 31470197), by the Department of Science and Technology of Guangdong Province, China (grants 2013B020302002 and 2013B051000043), by the Science Foundation of the State Key Laboratory of Biocontrol (grant SKLBC201123), and by the Guangdong Key Laboratory of Plant Resources.

References

Anderson JC, Pascuzzi PE, Xiao F, Sessa G, Martin GB. 2006. Host-mediated phosphorylation of type III effector AvrPto promotes *Pseudomonas* virulence and avirulence in tomato. The Plant Cell **18,** 502–514.

Bartsev AV, Boukli NM, Deakin WJ, Staehelin C, Broughton WJ. 2003. Purification and phosphorylation of the effector protein NopL from *Rhizobium* sp. NGR234. FEBS Letters **554,** 271–274.

Bartsev AV, Deakin WJ, Boukli NM, McAlvin CB, Stacey G, Malnöe P, Broughton WJ, Staehelin C. 2004. NopL, an effector protein of *Rhizobium* sp. NGR234, thwarts activation of plant defense reactions. Plant Physiology **134,** 871–879.

Boller T, Felix G. 2009. A renaissance of elicitors: perception of microbe-associated molecular patterns and danger signals by pattern-recognition receptors. Annual Review of Plant Biology **60,** 379–406.

Bradford MM. 1976. A rapid and sensitive method for the quantitation of microgram quantities of protein utilizing the principle of protein–dye binding. Analytical Biochemistry **72,** 248–254.

Bücking-Throm E, Duntze W, Hartwell LH, Manney TR. 1973. Reversible arrest of haploid yeast cells in the initiation of DNA synthesis by a diffusible sex factor. Experimental Cell Research **76,** 99–110.

Chen S, Songkumarn P, Liu J, Wang GL. 2009 A versatile zero background T-vector system for gene cloning and functional genomics. Plant Physiology **150,** 1111–1121.

Citovsky V, Lee, LY, Vyas S, Glick E, Chen MH, Vainstein A, Gafni Y, Gelvin SB, Tzfira T. 2006. Subcellular localization of interacting proteins by bimolecular fluorescence complementation *in planta*. Journal of Molecular Biology **362,** 1120–1131.

Cole GM, Stone DE, Reed SI. 1990. Stoichiometry of G protein subunits affects the *Saccharomyces cerevisiae* mating pheromone signal transduction pathway. Molecular and Cellular Biology **10,** 510–517.

Cui HT, Wang YJ, Xue L, Chu JF, Yan CY, Fu JH, Chen MS, Innes RW, Zhou JM. 2010. *Pseudomonas syringae* effector protein AvrB perturbs *Arabidopsis* hormone signaling by activating MAP kinase 4. Cell Host and Microbe **7,** 164–175.

Dahan J, Pichereaux C, Rossignol M, Blanc S, Wendehenne D, Pugin A, Bouroue S. 2009. Activation of a nuclear-localized SIPK in tobacco cells challenged by cryptogein, an elicitor of plant defense reactions. Biochemical Journal **418,** 191–200.

Dai WJ, Zeng Y, Xie ZP, Staehelin C. 2008. Symbiosis-promoting and deleterious effects of NopT, a novel type 3 effector of *Rhizobium* sp. strain NGR234. Journal of Bacteriology **190,** 5101–5110.

Desveaux D, Singer AU, Wu AJ, McNulty BC, Musselwhite L, Nimchuk Z, Sondek J, Dangl JL. 2007. Type III effector activation via nucleotide binding, phosphorylation, and host target interaction. PLoS Pathogens **3,** e48.

Dombrecht B, Vanderleyden J, Michiels, J. 2001. Stable RK2-derived cloning vectors for the analysis of gene expression and gene function in Gram-negative bacteria. Molecular Plant-Microbe Interactions **14,** 426–430.

Fauvart M, Michiels J. 2008. Rhizobial secreted proteins as determinants of host specificity in the *Rhizobium*–legume symbiosis. FEMS Microbiology Letters **285,** 1–9.

Felix G, Meins F. 1985. Purification, immunoassay and characterization of an abundant, cytokinin-regulated polypeptide in cultured tobacco tissues: evidence the protein is a β-1,3-glucanase. Planta **164,** 423–428.

Feng F, Zhou JM. 2012. Plant–bacterial pathogen interactions mediated by type III effectors. Current Opinion in Plant Biology **15,** 469–476.

Ferguson BJ, Indrasumunar A, Hayashi S, Lin MH, Lin YH, Reid DE, Gresshoff PM. 2010. Molecular analysis of legume nodule development and autoregulation. Journal of Integrative Plant Biology **52,** 61–76.

Figurski DH, Helinski DR. 1979. Replication of an origin-containing derivative of plasmid RK2 dependent on a plasmid function provided in trans. Proceedings of the National Academy of Sciences, USA **76,** 1648–1652.

Fotiadis CT, Dimou M, Georgakopoulos DG, Katinakis P, Tampakaki AP. 2012. Functional characterization of NopT1 and NopT2, two type III effectors of *Bradyrhizobium japonicum*. FEMS Microbiology Letters **327,** 66–77.

Gassmann W, Bhattacharjee S. 2012. Effector-triggered immunity signaling: from gene-for-gene pathways to protein–protein interaction networks. Molecular Plant-Microbe Interactions **25,** 862–868.

Giska F, Lichocka M, Piechocki M, Dadlez M, Schmelzer E, Hennig J, Krzymowska M. 2013. Phosphorylation of HopQ1, a type III effector from *Pseudomonas syringae*, creates a binding site for host 14-3-3 proteins. Plant Physiology **161,** 2049–2061.

Hann DR, Gimenez-Ibanez S, Rathjen JP. 2010. Bacterial virulence effectors and their activities. Current Opinion in Plant Biology **13,** 388–393.

Hayashi T, Morohashi H, Hatakeyama M. 2013. Bacterial EPIYA effectors—where do they come from? What are they? Where are they going? Cellular Microbiology **15,** 377–385.

Hempel J, Zehner S, Göttfert M, Patschkowski T. 2009. Analysis of the secretome of the soybean symbiont *Bradyrhizobium japonicum*. Journal of Biotechnology **140,** 51–58.

Hicks SW, Galán JE. 2013. Exploitation of eukaryotic subcellular targeting mechanisms by bacterial effectors. Nature Reviews Microbiology **11,** 316–326.

Hilioti Z, Sabbagh W, Paliwal S, Bergmann A, Goncalves MD, Bardwell L, Levchenko A. 2008. Oscillatory phosphorylation of yeast Fus3 MAP kinase controls periodic gene expression and morphogenesis. Current Biology **18,** 1700–1706.

Hoehenwarter W, Thomas M, Nukarinen E, Egelhofer V, Röhrig H, Weckwerth W, Conrath U, Beckers GJ. 2013. Identification of novel *in vivo* MAP kinase substrates in *Arabidopsis thaliana* through use of tandem metal oxide affinity chromatography. Molecular and Cellular Proteomics **12,** 369–380.

Hoffman GA, Garrison TR, Dohlman HG. 2002. Analysis of RGS proteins in *Saccharomyces cerevisiae*. Methods in Enzymology **344,** 617–631.

Hollender CA, Liu ZC. 2010. Bimolecular fluorescence complementation (BiFC) assay for protein–protein interaction in onion cells using the helios gene gun. Journal of Visualized Experiments **40,** 1–3.

Ishihama N, Yoshioka H. 2012. Post-translational regulation of WRKY transcription factors in plant immunity. Current Opinion in Plant Biology **15,** 431–437.

Jiménez-Guerrero I, Pérez-Montaño F, Monreal JA, Preston GM, Fones H, Vioque B, Ollero FJ, López-Baena FJ. 2015. The *Sinorhizobium* (*Ensifer*) *fredii* HH103 type 3 secretion system suppresses early defense responses to effectively nodulate soybean. Molecular Plant-Microbe Interactions **28,** 790–799.

Jones JD, Dangl JL. 2006. The plant immune system. Nature **444,** 323–329.

Jones RM, Wu H, Wentworth C, Luo L, Collier-Hyams L, Neish AS. 2008. *Salmonella* AvrA coordinates suppression of host immune and apoptotic defenses via JNK pathway blockade. Cell Host and Microbe **3,** 233–244.

Kambara K, Ardissone S, Kobayashi H, Saad MM, Schumpp O, Broughton WJ, Deakin WJ. 2009. Rhizobia utilize pathogen-like effector proteins during symbiosis. Molecular Microbiology **71,** 92–106.

Kimbrel JA, Thomas WJ, Jiang Y, Creason AL, Thireault CA, Sachs JL, Chang JH. 2013. Mutualistic co-evolution of type III effector genes in *Sinorhizobium fredii* and *Bradyrhizobium japonicum*. PLoS Pathogens **9,** e1003204.

Lane MC, O'Toole PW, Moore SA. 2006. Molecular basis of the interaction between the flagellar export proteins FliI and FliH from *Helicobacter pylori*. Journal of Biological Chemistry **281,** 508–517.

Li H, Xu H, Zhou Y, Zhang J, Long C, Li S, Chen S, Zhou JM, Shao F. 2007. The phosphothreonine lyase activity of a bacterial type III effector family. Science **315,** 1000–1003.

Macho AP, Zipfel C. 2014. Plant PRRs and the activation of innate immune signaling. Molecular Cell **54,** 263–272.

Macho AP, Zipfel C. 2015. Targeting of plant pattern recognition receptor-triggered immunity by bacterial type-III secretion system effectors. Current Opinion in Microbiology **23,** 14–22.

Marfori M, Mynott A, Ellis JJ, Mehdi AM, Saunders NFW, Curmi PM, Forwood JK, Bodén M, Kobe B. 2011. Molecular basis for specificity of nuclear import and prediction of nuclear localization. Biochimica et Biophysica Acta **1813,** 1562–1577.

Marie C, Deakin WJ, Viprey V, Kopcińska J, Golinowski W, Krishnan HB, Perret X, Broughton WJ. 2003. Characterisation of Nops, nodulation outer proteins, secreted via the type III secretion system of NGR234. Molecular Plant-Microbe Interactions **16,** 743–751.

Meinhardt LW, Krishnan HB, Balatti PA, Pueppke SG. 1993. Molecular cloning and characterization of a sym plasmid locus that regulates cultivar-specific nodulation of soybean by *Rhizobium fredii* USDA257. Molecular Microbiology **9,** 17–29.

Meng X, Zhang S. 2013. MAPK cascades in plant disease resistance signaling. Annual Review of Phytopathology **51,** 245–266.

Menke FLH, Kang HG, Chen Z, Park JM, Kumar D, Klessig DF. 2005. Tobacco transcription factor WRKY1 is phosphorylated by the MAP kinase SIPK and mediates HR-like cell death in tobacco. Molecular Plant-Microbe Interactions **18,** 1027–1034.

Mukherjee S, Keitany G, Li Y, Wang Y, Ball HL, Goldsmith EJ, Orth K. 2006. *Yersinia* YopJ acetylates and inhibits kinase activation by blocking phosphorylation. Science **312,** 1211–1214.

Okazaki S, Kaneko T, Sato S, Saeki K. 2013. Hijacking of leguminous nodulation signaling by the rhizobial type III secretion system. Proceedings of the National Academy of Sciences, USA **110,** 17131–17136.

Okazaki S, Zehner S, Hempel J, Lang K, Göttfert M. 2009. Genetic organization and functional analysis of the type III secretion system of *Bradyrhizobium elkanii*. FEMS Microbiology Letters **295,** 88–95.

Oldroyd GE. 2013. Speak, friend, and enter: signalling systems that promote beneficial symbiotic associations in plants. Nature Reviews Microbiology **11,** 252–263.

Perret X, Staehelin C, Broughton WJ. 2000. Molecular basis of symbiotic promiscuity. Microbiology and Molecular Biology Reviews **64,** 180–201.

Prentki P, Krisch HM. 1984. In vitro insertional mutagenesis with a selectable DNA fragment. Gene **29,** 303–313.

Puppo A, Groten K, Bastian F, Carzaniga R, Soussi M, Lucas MM, de Felipe MR, Harrison J, Vanacker H, Foyer CH. 2005. Legume nodule senescence: roles for redox and hormone signalling in the orchestration of the natural aging process. New Phytologist **165,** 683–701.

Quandt J, Hynes MF. 1993. Versatile suicide vectors which allow direct selection for gene replacement in gram-negative bacteria. Gene **127,** 15–21.

Rost B, Yachdav G., Liu J. 2004. The PredictProtein server. Nucleic Acids Research **32,** W321–W326.

Schechter LM, Guenther J, Olcay EA, Jang SC, Krishnan HB. 2010. Translocation of NopP by *Sinorhizobium fredii* USDA257 into *Vigna unguiculata* root nodules. Applied and Environmental Microbiology **76,** 3758–3761.

Sharrocks AD, Yang SH, Galanis A. 2000. Docking domains and substrate-specificity determination for MAP kinases. Trends in Biochemical Sciences **25,** 448–453.

Shinshi H, Mohnen D, Meins F. 1987. Regulation of a plant pathogenesis-related enzyme: inhibition of chitinase and chitinase mRNA accumulation in cultured tobacco tissues by auxin and cytokinin. Proceedings of the National Academy of Sciences, USA **84,** 89–93.

Skorpil P, Saad MM, Boukli NM, Kobayashi H, Ares-Orpel F, Broughton WJ, Deakin WJ. 2005. NopP, a phosphorylated effector of *Rhizobium* sp. strain NGR234, is a major determinant of nodulation of the tropical legumes *Flemingia congesta* and *Tephrosia vogelii*. Molecular Microbiology **57,** 1304–1317.

Staehelin C, Forsberg LS, D'Haeze W, *et al*. 2006. Exo-oligosaccharides of *Rhizobium* sp. strain NGR234 are required for symbiosis with various legumes. Journal of Bacteriology **188,** 6168–6178.

Staehelin C, Krishnan HB. 2015. Nodulation outer proteins: double-edged swords of symbiotic rhizobia. Biochemical Journal **470,** 263–274.

Tamura K, Peterson D, Peterson N, Stecher G, Nei M, Kumar S. 2011. MEGA 5: molecular evolutionary genetics analysis using maximum likelihood, evolutionary distance, and maximum parsimony methods. Molecular Biology and Evolution **28,** 2731–2739.

Tanoue T, Adachi M, Moriguchi T, Nishida E. 2000. A conserved docking motif in MAP kinases common to substrates, activators and regulators. Nature Cell Biology **2,** 110–116.

Trosky JE, Li Y, Mukherjee S, Keitany G, Ball H, Orth K. 2007. VopA inhibits ATP binding by acetylating the catalytic loop of MAPK kinases. Journal of Biological Chemistry **282,** 34299–34305.

Tsukui T, Eda S, Kaneko T, *et al*. 2013. The type III secretion system of *Bradyrhizobium japonicum* USDA122 mediates symbiotic incompatibility with *Rj2* soybean plants. Applied and Environmental Microbiology **79,** 1048–1051.

Viprey V, Del Greco A, Golinowski W, Broughton WJ, Perret X. 1998. Symbiotic implications of type III protein secretion machinery in *Rhizobium*. Molecular Microbiology **28,** 1381–1389.

Wang Y, Li J, Hou S, Wang X, Li Y, Ren D, Chen S, Tang X, Zhou JM. 2010. A *Pseudomonas syringae* ADP-ribosyltransferase inhibits *Arabidopsis* mitogen-activated protein kinase kinases. The Plant Cell **22,** 2033–2044.

Wenzel M, Friedrich L, Göttfert M, Zehner S. 2010. The type III-secreted protein NopE1 affects symbiosis and exhibits a calcium-dependent autocleavage activity. Molecular Plant-Microbe Interactions **23,** 124–129.

Xiao F, Giavalisco P, Martin GB. 2007. *Pseudomonas syringae* type III effector AvrPtoB is phosphorylated in plant cells on serine 258, promoting its virulence activity. Journal of Biological Chemistry **282,** 30737–30744.

Xin DW, Liao S, Xie ZP, Hann DR, Steinle L, Boller T, Staehelin C. 2012. Functional analysis of NopM, a novel E3 ubiquitin ligase (NEL) domain effector of *Rhizobium* sp. strain NGR234. PLoS Pathogens **8,** e1002707.

Yang KY, Liu Y, Zhang S. 2001. Activation of a mitogen-activated protein kinase pathway is involved in disease resistance in tobacco. Proceedings of the National Academy of Sciences, USA **98,** 741–746.

Yang S, Tang F, Gao M, Krishnanc HB, Zhu H. 2010. R gene-controlled host specificity in the legume–rhizobia symbiosis. Proceedings of the National Academy of Sciences, USA **107,** 18735–18740.

Yeam I, Nguyen HP, Martin GB. 2010. Phosphorylation of the *Pseudomonas syringae* effector AvrPto is required for FLS2/BAK1-independent virulence activity and recognition by tobacco. The Plant Journal **61,** 16–24.

Zhang J, Shao F, Li Y, *et al*. 2007. A *Pseudomonas syringae* effector inactivates MAPKs to suppress PAMP-induced immunity in plants. Cell Host and Microbe **1,** 175–185.

Zhang L, Chen XJ, Lu HB, Xie ZP, Staehelin C. 2011. Functional analysis of the type 3 effector nodulation outer protein L (NopL) from *Rhizobium* sp. NGR234. Journal of Biological Chemistry **286,** 32178–32187.

Zhang S, Liu Y. 2001. Activation of salicylic acid-induced protein kinase, a mitogen-activated protein kinase, induces multiple defense responses in tobacco. The Plant Cell **13,** 1877–1889.

Zhao C, Nie H, Shen Q, Zhang S, Lukowitz W, Tang D. 2014. EDR1 physically interacts with MKK4/MKK5 and negatively regulates a MAP kinase cascade to modulate plant innate immunity. PLoS Genetics **10,** e1004389.

SUPPLEMENTARY DATA

(Ying-Ying Ge, Qi-Wang Xiang, Christian Wagner, Di Zhang, Zhi-Ping Xie and Christian Staehelin (2015). The type 3 effector NopL of *Sinorhizobium* sp. strain NGR234 is a MAP kinase substrate)

This file contains Table S1, Table S2, Figure S1, Figure S2, Figure S3 and Figure S4.

Table S1. Plasmids and strains used in this work

Plasmids /strains	Relevant characteristics*	Reference/source
Plasmids:		
pBluescript II SK (+)	High copy number ColE1-based phagemid, Amp^r	Stratagene (Agilent Technologies), Shanghai, China
pBS(T)-*NtMEK2*^{DD}	pBluescript T-vector derivative containing the coding region of the *NtMEK2* MAP kinase kinase gene of *Nicotiana tabacum* (accession number: AF325168) with T227D/S233D double point mutations, Amp^r	Zhang *et al.*, 2011
pBS-p*nopL*	pBluescript II SK derivative carrying a *Kpn*I-*Bam*HI fragment amplified from pNGR234a containing the *nopL* promoter region (258 bp upstream of *nopL* start codon) and the coding region of *nopL*, Amp^r	Zhang *et al.*, 2011

pBS-*nopL*p-N	pBS-p*nopL* derivative containing a *Nco*I restriction site (start codon of the *nopL* coding region) introduced by site-directed mutagenesis with primers 26 and 27, Amp^r	This study
pBS-*nopL*p-N(E)	pBS-*nopL*p-N derivative without *Eco*RI restriction site (at the nucleotide position 922 bp in the *nopL* coding region) obtained by site-directed mutagenesis with primers 28 and 29, Amp^r	This study
pBS-*nopL*p-N-E	pBS-*nopL*p-N(E) derivative with created *Eco*RI restriction site (at nucleotide position 150 bp in the *nopL* coding region) obtained by site-directed mutagenesis with primers 30 and 31, Amp^r	This study
pMD18(T)	A TA cloning vector constructed from pUC18 with a disrupted multiple cloning site.	TaKaRa Biotechnology Co., Dalian, China
pMD18(T)-*nopL314*^{Mut}	pMD18-T derivative carrying a synthesized *Eco*RV-*Asc*I fragment (314 bp) of *nopL* containing five serine-to-alanin substitutions (S7A/S12A/S17A/S36A/S89A) and a mutation (t297c) for generation of a *Sma*I site, Amp^r Nucleotide sequence of the 314-bp fragment: gatatcaattcaaccgccccactaaacgcagccccacagccggacgctccaccacccgccaacgcgagtgcatttgcgc atcagctgagcggatttcaatatgcacctccacatgccgctgactcactattgccgcaggttgaagccgattccccatatttg acaccaggcatccctactcgcagtatttggattcggcatatccttatccatcaccttgtgaatggcagcatgacctgtatacca gggactagggaaagggctccccatcctagcgagcagcgaccgcatgcccgggtgctacagggcgcgcc	Constructed by Invitrogen (Thermo Fisher Scientific), Shanghai, China
pBS-*nopL*(S240A/S245A)	pBluescript II SK derivative carrying a *Bam*HI-*Xba*I fragment containing the coding region of *nopL* with S240A/S245A point mutations; insert amplified from pYES-*nopL*(S240A/S245A) using primers 15 and 16, Amp^r	This study

pBS-*nopL314*^{Mut} (S240A/S245A)	pBS-*nopL* (S240A/S245A) derivative with a replaced 314-bp *Eco*RV-*Asc*I fragment of *nopL* containing S7A/S12A/S17A/S36A/S89A mutations, Amp^r	This study
pBS-*nopL*(S12xA)	pBS-*nopL314*^{Mut} (S240A/S245A) derivative containing S73A/S139A/S148A/S187A/S198A point mutations introduced by site-directed mutagenesis using primers 1 to 10, Amp^r	This study
pBS-p*nopL-nopL*(S12xA)	pBS-*nopL*p-N-E derivative carrying an *Nco*I-*Bam*HI fragment containing the coding region of *nopL*(S12xA) amplified from pBS-*nopL*(S12xA) using primers 11and 12, Amp^r	This study
pHP45	Vector containing a 2-kb spectinomycin Ω cassette, Amp^r, Spe^r	Prentki and Krisch, 1984
pBS-p*nopL-nopL*(S12xA)-*spe*	pBS-p*nopL-nopL*(S12xA) derivative containing the 2-kb spectinomycin Ω cassette from pHP45 inserted into the *Bam*HI site, Amp^r, Spe^r	This study
pBS-*nopL*(S4xA)	pBS-p*nopL* derivative with S89A/S139A/S148A/S198A point mutations in the coding sequence of *nopL* obtained by site-directed mutagenesis using primers 3, 4, 5, 6, 9, 10, 13 and 14, Amp^r	This study
pBS-*nopL*(S6xA)	pBS-*nopL*p-N-E derivative carrying an *Nco*I-*Xba*I fragment containing the 4 point mutations of pBS-*nopL*(S4xA) and 2 additional point mutations (S73A/S187A); amplified from pBS-*nopL*(S4xA) by overlap PCR using primers 49, 50, 51, 52, 53 and 54, Amp^r	This study
pBS-*nopL*(S8xA)	pBS-*nopL*p-N-E derivative carrying an *Nco*I-*Xba*I fragment containing the six point	This study

	mutations of pBS-*nopL*(S6xA) and 2 additional point mutations (S17A/S36A); amplified from pBS-*nopL*(S6xA) and pBS-p*nopL*-*nopL*(S12xA)-*spe* by overlap PCR using primers 50, 51, 52 and 55, Amp^r	
pBS-*nopL*(S10xA)	pBS-*nopL*p-N-E derivative carrying an *Nco*I-*Xba*I fragment containing the the 8 point mutations of pBS-*nopL*(S8xA) and two additional point mutations (S7A/S12A); amplified from pBS- *nopL*(S8xA) and pBS-p*nopL*-*nopL*(S12xA)-*spe* by overlap PCR using primers 49, 50, 51 and 52, Amp^r	This study
pBS-*nopL*(S14xA)	pBS-*nopL*(S12xA) derivative with S52A/S250A point mutations in the coding sequence of *nopL* obtained by site-directed mutagenesis using primers 17 to 20, Amp^r	This study
pFAJ1702	A stable RK2-derived cloning vector, Amp^r, Tc^r	Dombrecht *et al.*, 2001
pFAJ-*nopL*	pFAJ1702 derivative carrying a *Kpn*I-*Bam*HI fragment amplified from *Sinorhizobium* sp. NGR234 containing the *nopL* promoter region (258 bp upstream of the *nopL* start codon) and the coding region of *nopL*, Tc^r	This study
pFAJ-*nopL*(S4xA)	pFAJ1702 derivative carrying a *Kpn*I-*Xba*I fragment containing the *nopL* promoter region and the coding region of *nopL*(S4xA), excised from pBS-*nopL*(S4xA), Tc^r	This study
pFAJ-*nopL*(S6xA)	pFAJ1702 derivative carrying a *Kpn*I-*Xba*I fragment containing the *nopL* promoter region and the coding region of *nopL*(S6xA) excised from pBS-*nopL*(S6xA), Tc^r	This study
pFAJ-*nopL*(S8xA)	pFAJ1702 derivative carrying a *Kpn*I-*Xba*I fragment containing the *nopL* promoter	This study

	region and the coding region of *nopL*(S8xA) excised from pBS-*nopL*(S8xA), Tc^r	
pFAJ-*nopL*(S10xA)	pFAJ1702 derivative carrying a *Kpn*I-*Xba*I fragment containing the *nopL* promoter region and the coding region of *nopL*(S10xA) excised from pBS-*nopL*(S10xA), Tc^r	This study
pFAJ-*nopL*(S12xA)	pFAJ1702 derivative carrying a *Kpn*I-*Xba*I fragment containing the *nopL* promoter region and the coding region of *nopL*(S12xA) excised from pBS-p*nopL-nopL*(S12xA), Tc^r	This study
pJQ200-mp18	A suicide vector containing a P15A origin of replication (*ori*), *lacZα* system, a *sacB* gene for sucrose selection and a *mob* gene for mobilization, Gm^r	Quandt and Hynes, 1993
pJQ-*y4mN*	pJQ200-mp18 digested with *Sma*I and *Sal*I containing a 1.5-kb fragment with the coding region of *y4mN* (accession number: NP_443980) PCR-amplified using genomic DNA of NGR234 as template, Gm^r	Liang, 2012
pJQ-*y4mN*-p*nopL-nopL*(S12xA)-*spe*	pJQ-*y4mN* derivative carrying a 3-kb fragment containing the *nopL* promoter region (258 bp upstream of the *nopL* start codon), the coding region of *nopL*(S12xA) and a spectinomycin Ω cassette excised from pBS-p*nopL-nopL*(S12xA)-*spe* with *Xba*I and inserted at the *Xba*I restriction site of *y4mN*, Gm^r, Spe^r	This study
pESC-Leu	Yeast protein expression vector with a galactose-inducible promoter (GAL1) and a *LEU* gene as selective marker, Amp^r	Stratagene (Agilent Technologies), Shanghai, China
pESC-*nopL*	pESC-Leu derivative carrying a *Bam*HI-*Hin*dIII fragment containing the coding region of *nopL* amplified from pBS-p*nopL* using primers 21 and 22, Amp^r	This study

pESC-*nopL*(S12xA)	pESC-Leu derivative carrying a *Bam*HI-*Hin*dIII fragment containing the coding region of *nopL*(S12xA) amplified from pBS-*nopL*(S12xA) using primers 22 and 23, Amp^r	This study
pESC-*nopL*(S4xA)	pESC-Leu derivative carrying a *Bam*HI-*Hin*dIII fragment containing the coding region of *nopL*(S4xA) amplified from pBS-p*nopL*(S4xA) using primers 21 and 22, Amp^r	This study
pESC-*nopL*(S14xA)	pESC-Leu derivative carrying a *Bam*HI-*Hin*dIII fragment containing the coding region of *nopL*(S14xA) amplified from pBS-p*nopL*(S14xA) using primers 22 and 23, Amp^r	This study
pYES2	Yeast protein expression vector with a galactose-inducible promoter (GAL1), 2μ origin and the *URA3* gene as selectable marker, Amp^r	Invitrogen (Thermo Fisher Scientific)
pYES-*nopL*	A 1-kb fragment containing the coding region of *nopL* amplified from *Sinorhizobium* sp. NGR234 (accession number NC_000914) and cloned into the *Bam*HI-*Xba*I sites of pYES2, Amp^r	Zhang *et al.*, 2011
pYES-*nopL*(S240A/S245A)	pYES-*nopL* derivative containing two point mutations (S240A/S245A in *nopL*), Amp^r	Zhang *et al.*, 2011
pYES-*nopL*(S12xA)	pYES2 derivative carrying a *Bam*HI-*Xho*I fragment containing the coding region of *nopL*(S12xA) amplified from pBS-*nopL*(S12xA) using primers 24 and 25, Amp^r	This study
pX-DR	pBluescript II SK derivative containing the cauliflower mosaic virus (CaMV) 35S promoter, the coding sequence of *DsRed*, the negative selection gene marker *ccdB* (inserted between two *Xcm*I restriction sites) and the nopalin synthase terminator (Tnos), Amp^r	Chen *et al.*, 2009; kindly provided by Prof. Guo-Liang Wang, Hunan Agricultural

		University, Changsha, China
pX-DR-*nopL*	pX-DR derivative containing the coding region of *nopL* inserted into the *Xcm*I restriction site by T/A cloning; insert amplified from pBS-p*nopL* using primers 32 and 33, Amp^r	This study
pX-DR-*nopL*(S12xA)	pX-DR derivative containing the coding region of *nopL*(S12xA) inserted into the *Xcm*I restriction site by T/A cloning; insert amplified from pBS-*nopL*(S12xA) using primers 32 and 33, Amp^r	This study
pCAMBIA-1302	Binary vector with the CaMV 35S promoter and the coding sequence of *gfp*, Km^r	Cambia, Brisbane, Australia
pCAMBIA-*nopL*	pCAMBIA-1302 derivative containing the coding region of *nopL* inserted between the *Nco*I and *Spe*I restriction sites at the N-terminus of the *gfp* gene; insert amplified from pBS-p*nopL* using primers 34 and 35, Km^r	This study
pCAMBIA-*nopL*(S12xA)	pCAMBIA-1302 derivative containing the coding region of *nopL*(S12xA) inserted between the *Nco*I and *Spe*I restriction sites at the N-terminus of the *gfp* gene; insert amplified from pBS-*nopL*(S12xA) using primers 11 and 35, Km^r	This study
pSAT1-nEYFP-N1	Bi-molecular fluorescence complementation vector with the CaMV 35S promoter and a multiple cloning site in the N-terminus of the coding region of nEYFP (accession number: DQ169001), Amp^r	Arabidopsis Biological Resource Center (http://arabidopsis.org/index.jsp)

pSAT1-cEYFP-N1	Bi-molecular fluorescence complementation vector with the CaMV 35S promoter, and a multiple cloning site in the N-terminus of the coding region of cEYFP (accession number: DQ169000), Amp^r	Arabidopsis Biological Resource Center (http://arabidopsis.org/index.jsp)
pSAT1-nEYFP-N1-*nopL*	pSAT1-nEYFP-N1 derivative containing the coding region of *nopL* inserted between the *Hin*dIII and *Bam*HI restriction sites; insert amplified from pBS-p*nopL* using primers 36 and 37, Amp^r	This study
pSAT1-nEYFP-N1-*nopL*(S12xA)	pSAT1-nEYFP-N1 derivative containing the coding region of *nopL*(S12xA) inserted between the *Hin*d III and *Bam*H I restriction sites; insert amplified from pBS-*nopL*(S12xA) using primers 38 and 37, Amp^r	This study
pSAT1-cEYFP-N1-*SIPK*	pSAT1-cEYFP-N1 derivative containing the coding region of *SIPK* of *Nicotiana tabacum* (accession number: U94192) inserted between *Bam*H I and *Eco*R I restriction sites; insert amplified from pET-*SIPK* using primers 39 and 40, Amp^r	This study
pGEX-4T-1	Expression vector for GST-fusion proteins, Amp^r	Amersham Biosciences/GE Healthcare, Buckinghamshire, UK)
pGEX-*nopL*	pGEX-4T-1 derivative containing the coding region of *nopL* inserted between *Bam*H I and *Sal* I restriction sites, Amp^r	Zhang *et al.*, 2011
pGEX-*nopL*(S12xA)	pGEX-4T-1 derivative containing the coding region of *nopL*(S12xA) inserted between	This study

	*Bam*H I and *Sal* I restriction sites; insert amplified from pBS-*nopL*(S12xA) using primers 41 and 42, Amp^r	
pGEX-*SIPK*	pGEX-4T-1 derivative containing the coding region of *Nicotiana tobacum SIPK* gene (accession number: U94192) inserted between *Bam*H I and *Eco*R I restriction sites; insert amplified from pET-*SIPK* using primers 39 and 40, Amp^r	This study
pGEX-*NtMEK2*^{DD}	pGEX-4T-1 derivative containing coding the region of *Nicotiana tobacum NtMEK2*^{DD} (accession number: AF325168) inserted between *Sma* I and *Not* I restriction sites; insert amplified from pBS(T)-*NtMEK2*^{DD} using primers 41 and 42, Amp^r	This study
pET28b	Expression vector for His-tag fusion proteins based on pBR322, Km^r	Novagen (Merck Chemicals) Darmstadt, Germany
pET-*NtMEK2*^{DD}	pET28b derivative carrying an *Nco* I-*Hin*d III fragment containing the coding region of *NtMEK2*^{DD} amplified from pBS(T)-*NtMEK2*^{DD} fused to a C-terminal 6×His tag using primers 43 and 44, Km^r	This study
pET-*SIPK*	pET28b derivative carrying a *Bam*HI-*Xho*I fragment containing the coding region of *SIPK* of *N. tabacum* (accession number: U94192) fused to an N-terminal 6×His tag, Km^r	Zhang *et al.*, 2011
pPROEX-*nopL*	pPROEX-1 (expression vector for His-tag fusion proteins; BRL Life Technologies, Rockville, MD, USA) derivative carrying an *Ehe*I-*Xba*I fragment containing the coding region of *nopL* gene fused to an N-terminal 6×His tag, Amp^r	Bartsev *et al.*, 2003
pPROEX-*nopL*(S12xA)	pPROEX-1 derivative carrying a *Ehe*I-*Bam*HI fragment containing the coding region of *nopL*(S12xA) fused to an N-terminal 6×His tag; insert amplified from	This study

	pBS-*nopL*(S12xA) using primers 45, 12, Amp^r	
pPZP112	Binary vector for *Agrobacterium*-mediated plant transformation, contains left border and right border sequences of T-DNA, Km^r for plant selection, Cm^r	Hajdukiewicz *et al.*, 1994
pPZP-*nopL*	pPZP112 derivative containing *nopL* and the CaMV 35S promoter, Cm^r	Bartsev *et al.*, 2004
pRT104	High copy vector carrying the CaMV 35S promoter, a polyadenylation signal and a modified polylinker of pUC18/19.	Töpfer *et al.*, 1987
pRT-*nopL*(S12xA)	pRT104 derivative carrying the *Nco*I-*Xba*I fragment containing the coding region of *nopL*(S12xA) amplified from pBS-*nopL*(S12xA) using primers 11, 46, Amp^r	This study
pPZP-*nopL*(S12xA)	pPZP112 derivative carrying the *Hin*dIII fragment excised from pRT-*nopL*(S12xA), Cm^r	This study
Strains: *Escherichia coli* DH5α	*supE44* Δ*lac*U169 (*ϕ*80*lacZ*ΔM15) *hsdR17 recA1 endA1 gyrA96 thi-1 relA1*	GIBCO BRL, Bethesda, MD, USA
BL21 (DE3)	F$^-$ *ompT hsdS*$_B$ (r_B^- m_B^-) *gal dcm* (DE3)	Novagen (Merck Chemicals), Darmstadt, Germany

Sinorhizobium sp. NGR234	*Sinorhizobium* (*Ensifer, Rhizobium*) sp. strain NGR234 isolated from *Lablab purpureus* (Rif^r derivative) , Rif^r	Trinick, 1980
NGRΩ*nopL*	NGR234 derivative containing an Ω cassette inserted into the *Eco*RV site of *nopL*, Rif^r, Km^r	Marie *et al.*, 2003
NGRΩ*nopL*-*nopL*(S12xA)	NGRΩ*nopL* derivative carrying a DNA fragment inserted into the *Xba*I site of *y4mN* containing the *nopL* promoter region (258 bp upstream of *nopL* start codon, amplified from NGR234), the coding region of *nopL*(S12xA) and a spectinomycin Ω cassette, Rif^r, Km^r, Spe^r	This work
NGRΩ*nopL* pFAJ1702	NGRΩ*nopL* derivative carrying pFAJ1702, Rif^r, Km^r, Tc^r	This work
NGRΩ*nopL* pFAJ-*nopL*	NGRΩ*nopL* derivative carrying pFAJ-*nopL*, Rif^r, Km^r, Tc^r	This work
NGRΩ*nopL* pFAJ-*nopL*(S4xA)	NGRΩ*nopL* derivative carrying pFAJ-*nopL*(S4xA), Rif^r, Km^r, Tc^r	This work
NGRΩ*nopL* pFAJ-*nopL*(S6xA)	NGRΩ*nopL* derivative carrying pFAJ-*nopL*(S6xA), Rif^r, Km^r, Tc^r	This work
NGRΩ*nopL* pFAJ-*nopL*(S8xA)	NGRΩ*nopL* derivative carrying pFAJ-*nopL*(S8xA), Rif^r, Km^r, Tc^r	This work
NGRΩ*nopL* pFAJ-*nopL*(S10xA)	NGRΩ*nopL* derivative carrying pFAJ-*nopL*(S10xA), Rif^r, Km^r, Tc^r	This work
NGRΩ*nopL* pFAJ-*nopL*(S12xA)	NGRΩ*nopL* derivative carrying pFAJ-*nopL*(S12xA), Rif^r, Km^r, Tc^r	This work
Saccharomyces cerevisiae W303-1A	*MAT*a *ade2-1 can1-100 his3-11,15 leu2-3,112 rad5-535 trp1-1 ura3-1*	Wallis *et al.*, 1989

W303-1B	*MATα ade2-1 can1-100 his3-11,15 leu2-3,112 rad5-535 trp1-1 ura3-1*	Kindly provided by Prof. Yong-Jun Lu, Sun Yat-sen University, Guangzhou, China
SY2227	*MAT*a *ade1-1 leu2-2,113 trp1 ura3-52 bar1 HIS3::pFUS1::HIS3 mfa2-Δ1::FUS1-lacZ rad16::pGAL1::STE4*	Edwards *et al.*, 1997
Agrobacterium tumefaciens		
AGL1	pTiB0542, disarmed C58 (chromosomal), hypervirulent strain for plant transformation, Cb^r	Lazo *et al.*, 1991
pPZP-*nopL*(S12xA)	pPZP112 derivative carrying the *Hin*dIII fragment excised from pRT-*nopL*(S12xA), Cm^r	This study

*Amp^r, Cm^r, Km^r, Rif^r, Tc^r, Spe^r, resistance to ampicillin, chloramphenicol, kanamycin, rifampin, tetracycline and spectinomycin, respectively.

References cited in Table S1

1. **Bartsev, A.V., Boukli, N.M., Deakin, W.J., Staehelin, C. and Broughton, W.J.** (2003) Purification and phosphorylation of the effector protein NopL from *Rhizobium* sp. NGR234. *FEBS Lett.* **554**, 271–274.
2. **Bartsev, A.V., Deakin, W.J., Boukli, N.M., McAlvin, C.B., Stacey, G., Malnoë, P., Broughton, W.J. and Staehelin, C.** (2004) NopL, an effector protein of *Rhizobium* sp. NGR234, thwarts activation of plant defense reactions. *Plant Physiol.* **134**, 871–879.

3. **Chen, S.B., Songkumarn, P., Liu, J.L. and Wang, G.L.** (2009) A versatile zero background T-vector system for gene cloning and functional genomics. *Plant Physiol.* **150**, 1111–1121.
4. **Dombrecht, B., Vanderleyden, J. and Michiels, J.** (2001) Stable RK2-derived cloning vectors for the analysis of gene expression and gene function in gram-negative bacteria. *Mol. Plant Microbe Interact.* **14**, 426-30.
5. **Edwards, M.C., Liegeois, N., Horecka, J., DePinho, R.A., Sprague, G.F., Tyers, M. and Elledge, S.J.** (1997) Human *CPR* (cell cycle progression restoration) genes impart a Far$^-$ phenotype on yeast cells. *Genetics* **147**, 1063–1076.
6. **Hajdukiewicz, P., Svab, Z. and Maliga, P.** (1994) The small, versatile *pPZP* family *Agrobacterium* binary vectors for plant transformation. *Plant Mol. Biol.* **25**, 989–994.
7. **Lazo, G.R., Stein, P.A. and Ludwig, R.A.** (1991) A DNA transformation–competent *Arabidopsis* genomic library in *Agrobacterium*. *Biotechnology* (*NY*) **9**, 963–967.
8. **Liang, M.T.** (2012) Use of the Cre-loxP recombination system in interactions between *Rhizobium*/*Agrobacterium* and host plants. Doctoral dissertation, Sun Yat-sen University, Guangzhou, China.
9. **Marie, C., Deakin, W.J., Viprey, V., Kopciñsk,a J., Golinowski, W., Krishnan, H.B., Perret, X. and Broughton, W.J.** (2003) Characterisation of Nops, nodulation outer proteins, secreted via the type III secretion system of NGR234. *Mol. Plant Microbe Interact.* **16**, 743–751.
10. **Prentki, P. and Krisch, H.M.** (1984) *In vitro* insertional mutagenesis with a selectable DNA fragment. Gene **29**, 293–303.
11. **Quandt, J. and Hynes, M.F.** (1993) Versatile suicide vectors which allow direct selection for gene replacement in Gram-negative bacteria. *Gene* **127**, 15–21.
12. **Töpfer, R., Matzeit, V., Gronenborn, B., Schell, J. and Steinbiss, H.H.** (1987) A set of plant expression vectors for transcriptional and translational fusions. *Nucleic Acids Res.* **15**, 5890.
13. **Trinick, M.J.** (1980) Relationships amongst the fast-growing rhizobia of *Lablab purpureus*, *Leucaena leucocephala*, *Mimosa* spp., *Acacia farnesiana* and *Sesbania grandiflora* and their affinities with other rhizobial groups. *J. Appl. Bacteriol.* **49**, 39–53.
14. **Wallis, J.W., Chrebet, G., Brodsky, G., Rolfe, M. and Rothstein, R.** (1989) A hyper-recombination mutation in *S. cerevisiae* identifies a novel eukaryotic topoisomerase. *Cell* **58**, 409–419.
15. **Zhang, L., Chen, X.J., Lu, H.B., Xie, Z.P. and Staehelin, C.** (2011). Functional analysis of the type 3 effector nodulation outer protein L (NopL) from *Rhizobium* sp. NGR234. *J. Biol. Chem.* **286**, 32178–32187.

Table S2. Primers used in this study

No	Sequence (5' to 3')	Restriction site	Description
1	catatccttatccagcaccttgtgaatgg		Site-directed mutagenesis; for construction of pBS-*nopL* (S8xA).
2	ccattcacaaggtgctggataaggatatg		
3	tcgcaagccgggctagccccgtccgccaccc		Site-directed mutagenesis; for construction of pBS-*nopL*(S9xA) and pBS-*nopL*(S139A/S148A/S198A).
4	gggtggcggacggggctagcccggcttgcga		
5	accccactgaacccagccccaccgccgcatgc		Site-directed mutagenesis; for construction of pBS-*nopL*(S10xA) and pBS-p*nopL*(S148A/S198A).
6	gcatgcggcggtggggctgggttcagtggggt		
7	acgcgggctacagctgctcccgcgccactga		Site-directed mutagenesis; for construction of pBS-*nopL*(S11xA).
8	tcagtggcgcgggagcagctgtagcccgcgt		
9	gctgagaggggaagggctccccagcctagcg		Site-directed mutagenesis; for construction of pBS-*nopL*(S12xA) and pBS-p*nopL*(S198A).
10	cgctaggctggggagcccttcccctctcagc		
11	ggccatggat atggatatcaattcaaccgc	*Nco*I	For construction of pBS-p*nopL-nopL*(S12xA).
12	gcggatcc tcaaatgtcaaaatccaccg	*Bam*HI	
13	aggactagggaaagggctccccatcctagcg		Site-directed mutagenesis; for construction of

14	cgctaggatggggagccctttccctagtcct		pBS-p*nopL*(S4xA).
15	ggggatcc atggatatcaattcaaccag	*Bam*HI	For construction of pBS-*nopL* (S240A/S245A).
16	ggtctaga tcaaatgtcaaaatccaccg	*Xba*I	
17	gcaggttgaagccgatgccccatatttggacac		Site-directed mutagenesis; for construction of pBS-*nopL*(S13xA).
18	gtgtccaaatatggggcatcggcttcaacctgc		
19	ccgtcgcaagcccggccagcgcacgcttggccgtcctc		Site-directed mutagenesis; for construction of pBS-*nopL*(S14xA).
20	gaggacggccaagcgtgcgctggccgggcttgcgacgg		
21	gcggatccg atggatatcaattcaaccag	*Bam*HI	For construction of pESC-*nopL*.
22	gcaagctt tcaaatgtcaaaatccaccg	*Hin*dIII	
23	gcggatccg atggatatcaattcaaccgccccactaaa	*Bam*HI	For construction of pESC-*nopL*(S12xA).
24	cgggatcc atggatatcaattcaac	*Bam*HI	For construction of pYES-*nopL*(S12xA).
25	gcctcgag tcaaatgtcaaaatccaccg	*Xho*I	
26	tcaaaggagaaacaccatggatatcaattc	*Nco*I	Site-directed mutagenesis; for construction of pBS-*nopL*p-N.
27	gaattgatatccatggtgtttctcctttga		
28	gcaggttgaagccatgaattcccatatttg	*Eco*RI	Site-directed mutagenesis; for construction of pBS-*nopL*p-N(E).
29	caaatatggggaattcatggcttcaacctgc		
30	cacgttgccgaatttcgaggcgagggagt		Site-directed mutagenesis; for construction of pBS-*nopL*p-N-E.
31	actccctcgcctcgaaattcggcaacgtg		

32 33	a atggatatcaattcaaccagc tcaaatgtcaaaatccaccg		For construction of pX-DR-*nopL*.
34 35	cgccatggat atggatatcaattcaaccag cgactagt tcaaatgtcaaaatccaccg	*Nco*I *Spe*I	For construction of pCAMBIA-*nopL*.
36 37	cgaagctt atggatatcaattcaaccagc gcggatcc tcaaatgtcaaaatccaccgatggcctga	*Hin*dIII *Bam*HI	For construction of pSAT1-nEYFP-N1-*nopL*.
38	cgaagctt atggatatcaattcaaccgc	*Hin*dIII	For construction of pSAT1-nEYFP-N1-*nopL*(S12xA).
39 40	gcggatcc atggatggttctggtcagcagacggac gcgaattc tggtattcaggattaaatgcaagcgactccctg	*Bam*HI *Eco*RI	For construction of pSAT1-nEYFP-N1-*SIPK*.
41 42	atacccggga atgcgacctcttcaaccacc atagcggccgc ttaagaagaaaaatgaggaggtg	*Sma*I *Not*I	For construction of pGEX-*NtMEK2*^{DD}.
43 44	ggccatggcg atgcgacctcttcaaccacccccaccagccgcc ggaagctt agaagaaaaatgaggaggtggaggtaa	*Nco*I *Hin*dIII	For construction of pET-*NtMEK2*^{DD}.
45	cggggcgcc atggatatcaattcaaccgc	*Ehe*I	For construction of pPROEX-*nopL*(S12xA).
46	gctctaga tcaaatgtcaaaatccaccgatg	*Xba*I	For construction of pRT-*nopL*(S12xA).

47 48	ccggttcctacaagctcgacaacc ctgtttctcctttgaaatatggaggccccaagcctttccgatgcg		Amplification of a 1.55-kb DNA fragment from pNGR234a; the amplicon contains 343-bp of *y4mO*, 946-bp of *y4mN* and 258-bp of the promoter region of *nopL*; used for confirmation of constructed mutant NGRΩ*nopL*-*nopL*(S12xA).
49	attCCatggatatcaattcaacc	*Nco*I	Site-directed mutagenesis (overlap PCR); for construction of pBS-*nopL*(S6xA)
50	TGCTCTAGAtcaaatgtcaaaat	*Xba*I	Site-directed mutagenesis (overlap PCR); for construction of pBS-*nopL*(S6xA)
51	catatccttatccaGcaccttgtgaatgg		Site-directed mutagenesis (S73; overlap PCR); for construction of pBS-*nopL*(S6xA)
52	ccattcacaaggtgCtggataaggatatg		Site-directed mutagenesis (S73; overlap PCR); for construction of pBS-*nopL*(S6xA)
53	gcgggctacagctGctcccgcgccactg		Site-directed mutagenesis (S187; overlap PCR); for construction of pBS-*nopL*(S6xA)
54	cagtggcgcgggagCagctgtagcccgc		Site-directed mutagenesis (S187; overlap PCR); for construction of pBS-*nopL*(S6xA)

54	attccatggatatcaattcaaccagcccactaaacgcaagcccacagcc ggac	*Nco*I	Amplification of a *nopL*(S10xA) fragment from pBS-*nopL*(S12xA); for construction of pBS-*nopL*(S10xA).

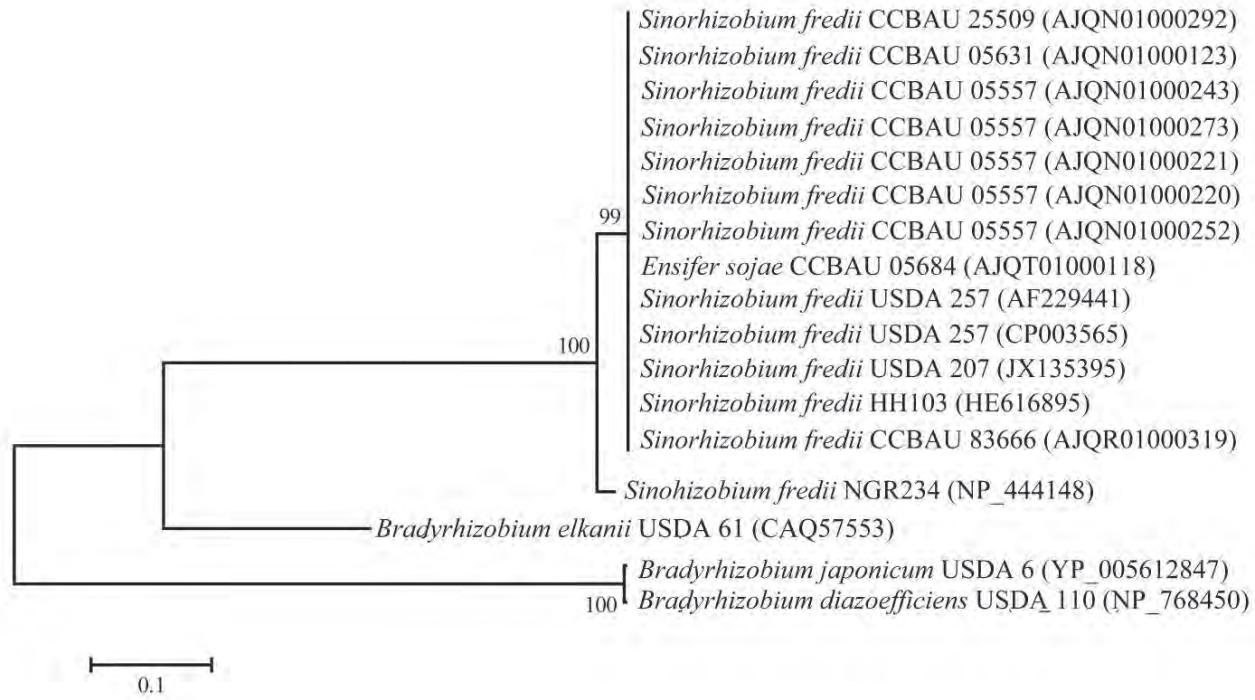

Figure S1. Phylogenic tree of the NopL effector family. The tree deduced from predicted amino acid sequences was constructed with the MEGA 5 program using the neighbor-joining method. The horizontal bar represents a distance of 0.1 substitution per site. Note: *Sinorhizobium fredii* NGR234 is synonymous with *Rhizobium* (*Ensifer*) sp. NGR234 and *Bradyrhizobium diazoefficiens* USDA 110 with *Bradyrhizobium japonicum* USDA 110.

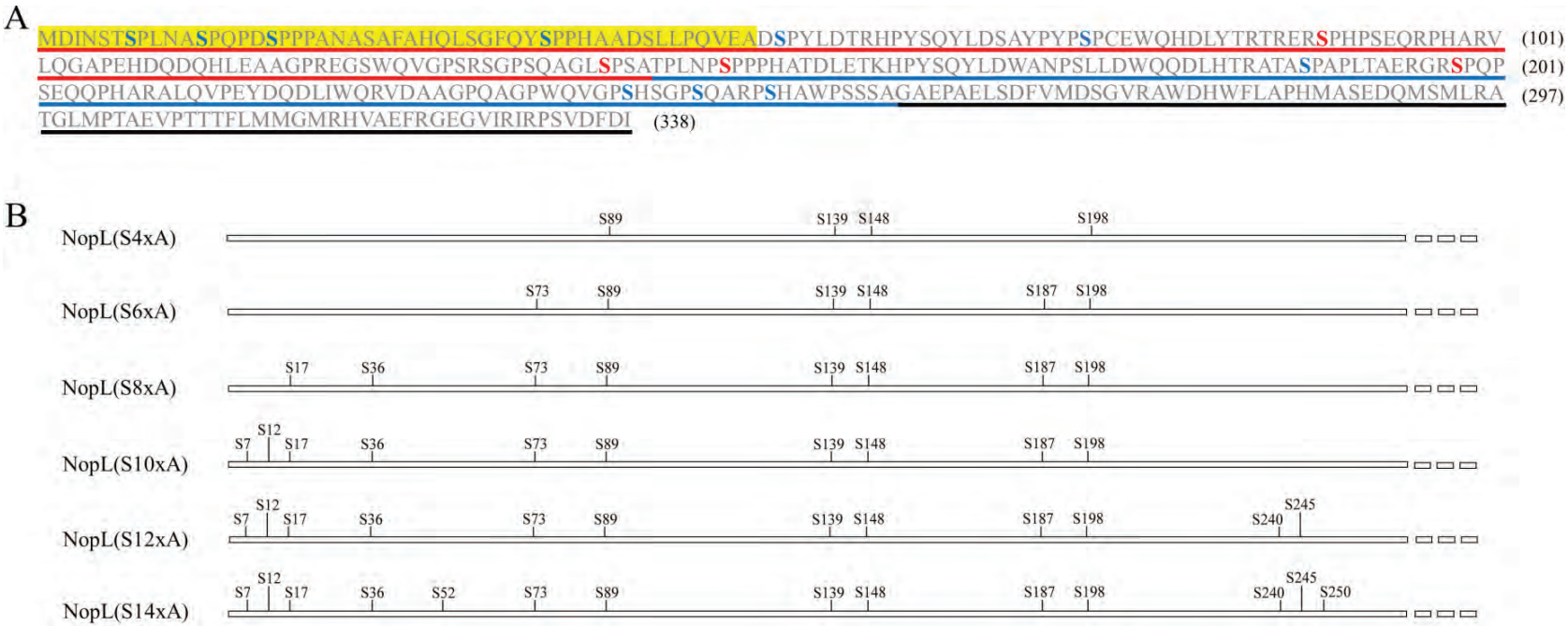

Figure S2. Serine-to-alanine substitutions in NopL analyzed in this study. (A) The NopL protein of *Sinorhizobium* sp. NGR234 consists of a predicted N-terminal secretion signal sequence (approximately 50 amino acids; highlighted in yellow), two repeats (underlined in red and blue, respectively) and a C-terminal domain (underlined in black). The previously identified four phospho-serine residues are marked in red. Additionally substituted serine residues are highlighted in blue (including those in the GPSHSGPSQARPSH motif at the end of the second repeat). Numbers at the end of each line indicate the position of the last amino acid. **(B)** Position of substituted serine residues in indicated NopL variants.

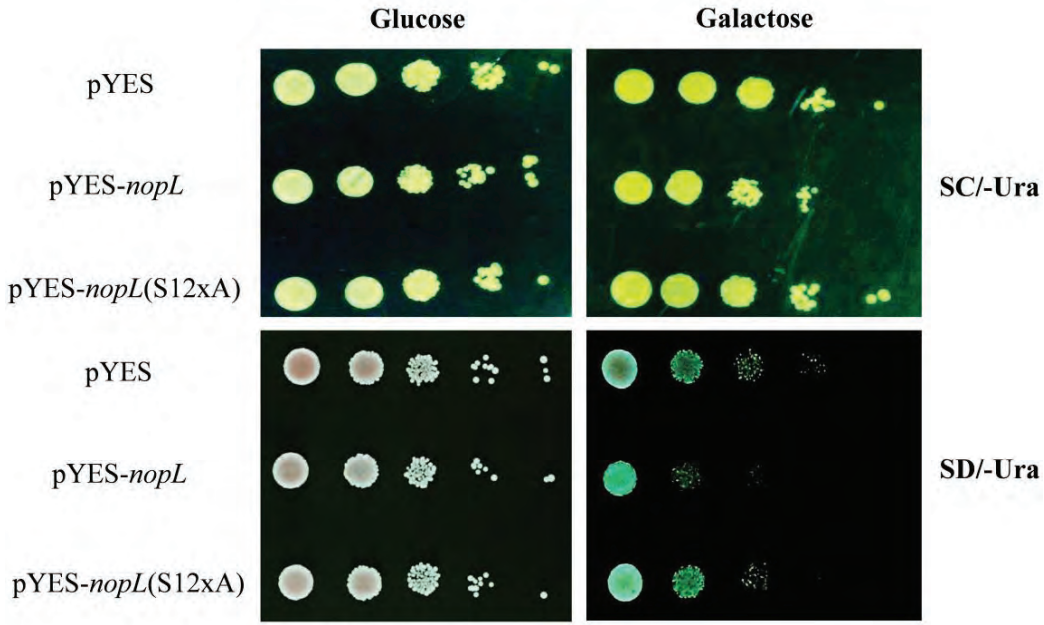

Figure S3. Expression of NopL and NopL(S12xA) in yeast strain W303-1B. Yeast cells carrying either pYES-*nopL* or pYES-*nopL*(S12xA) were grown on SD/-Ura or SC/-Ura medium plates supplemented with 2% (w/v) glucose or galactose as inducer. Cell suspensions (10 µl) were added in 10-fold serial dilutions, starting with an OD_{600} of 0.1. Photographs were taken 48 h (glucose plates) and 60 h (galactose plates) after inoculation. Expression of NopL but not NopL(S12xA) in yeast grown on galactose plates resulted in delayed formation of colonies.

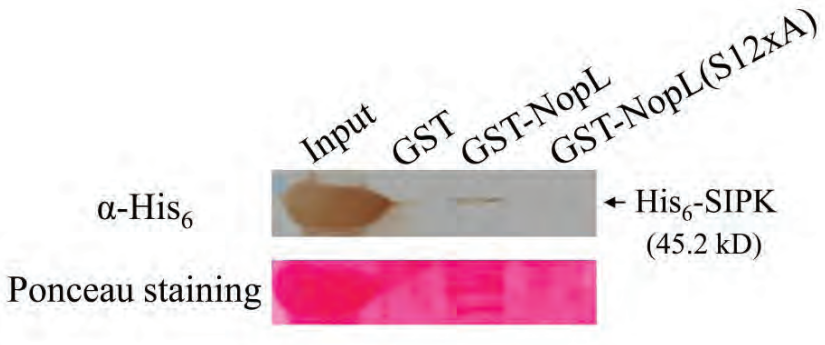

Figure S4. Pull-down assay. His-tagged SIPK (His_6-SIPK) was used as prey and glutathione S-transferase (GST) tagged NopL proteins as bait (GST-NopL and GST-NopL(S12xA), respectively). Purified GST served as a control. Formed protein complexes were immobilized on glutathione agarose beads. Eluted proteins were separated by SDS-PAGE. His_6-SIPK was detected by Western blot analysis with an anti-His_6 antibody and by Ponceau staining. "Input" represents the total amount of His_6-SIPK used in the assay.